



**CZECH TECHNICAL UNIVERSITY IN PRAGUE**

---

**Faculty of Mechanical Engineering  
Department of Automotive, Combustion Engine and Railway Engineering**

## **Cylinder Head Gasket for an Experimental Single Cylinder Engine**

Diploma Thesis

Study program: N2307 Master of Automotive Engineering

Field of study: 2301T050 Advanced Powertrains

Thesis advisor: Ing. Jindřich Hořenín

**Lukáš Kubový**

---

**Prague 2017**

## DIPLOMA THESIS ASSIGNMENT

Student: **Bc. Lukáš KUBOVÝ**

Study program: **N2307 Master of Automotive Engineering**

Field of study: **2301T050 Advanced Powertrains**

School year: 2016/2017

Title: **Cylinder Head Gasket for an Experimental Single Cylinder Engine**

### Assignment:

Perform a literature search of contemporary cylinder head gasket designs. Perform an assessment of the appropriate gasket design for a one cylinder research engine with a cylinder unit of a SI automotive engine ŠKODA with 74.5mm bore and 85.9 mm stroke. Modify a design of the upper part of the cylinder block for the installation of the selected gasket.

Perform mechanical stress calculations:

- Required preload of the cylinder head screws
- Analyze stress of the upper mounting of the cylinder with the proposed gasket
- Perform thermal load calculations of the gasket:
  - Calculate temperature field of the cylinder liner and the cylinder block with the given cylinder head gasket.
  - Take over the thermal field of the cylinder head from Mgr. Svoboda, who handles the cylinder head design.

Perform calculations with respect to the maximum combustion pressure of 130 bar and a maximum engine speed of 7,000 rpm and according to the supplied full load map.

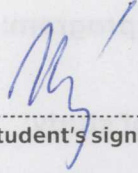
Create manufacturing documentation of the cylinder head gasket and its assembly. Modify the cylinder block manufacturing drawings with regard to the installation of the cylinder head gasket.


Thesis extent: minimally 55 pages  
Graphical extent:  
Specialized literature list:

Supervisor: Ing. Jindřich Hořenín  
Specialist:  
Date of thesis assignment: 21 March 2017  
Deadline of submission: 21 August 2017


*The student acknowledges that he/she must elaborate the project by himself/herself, without any help except consultations with his/her supervisor. A list of used literature, other sources and names of consultants must be listed in the thesis.*

I received the assignment on (date): 29.3.2017

  
-----  
Student's signature

  
-----  
Doc. Ing. Oldřich VÍTEK, Ph.D.

Head of Department

  
-----  
Prof. Ing. Michael VALÁŠEK, DrSc.

Dean



Prague, 10 March 2017

## **Declaration**

I declare that I have prepared this diploma thesis independently, under the supervision of Ing. Jindřich Hořenín and using the literature mentioned below.

In Prague on: .....

Signature: .....

## **Acknowledgements**

I would like to thank Ing. Jindřich Hořenín for his leadership and expert advice in writing this diploma thesis. Furthermore, I would like to thank Doc. Ing. Oldřich Vitek, Ph.D., Ing. Jiří Vávra, Ph.D., Ing. Milan Rudolf and other members of the development team at ŠKODA-AUTO a.s.

## Abstract

The aim of this work is to investigate the current possibilities of head gaskets of the experimental single-cylinder engine and propose an appropriate solution. The proposed solution contains the required preload of the cylinder head screws, stress analysis of the upper mounting of the cylinder with the proposed gasket, the temperature field of the cylinder liner and the cylinder block with the given cylinder head gasket. The manufacturing documentation of the engine block and cylinder liner is made with regard to the chosen gasket design.

**Keywords:** combustion engine, experimental engine, single cylinder engine, cylinder head gasket

## Abstrakt

Cílem této práce je průzkum současných možností utěsnění hlavy válce experimentálního jednoválcového motoru a navrhnout vhodné řešení těsnění hlavy válce. Navrhované řešení obsahuje požadované předpětí hlavových šroubů, analýzu napětí horního uložení válce s navrženým těsněním, teplotní pole vložky válce, bloku motoru a navrženého těsnění. Výrobní dokumentace vložky válce a bloku motoru je vytvořena s ohledem na zvolené těsnění.

**Klíčová slova:** spalovací motor, zkušební motor, jednoválcový motor, těsnění hlavy válce

# Table of contents

<b>Chapter 1: Introduction</b> .....	<b>12</b>
1.1 Experimental Single-Cylinder Engine .....	13
<b>Chapter 2: Head Gaskets Basics</b> .....	<b>15</b>
2.1 Composite Head Gaskets .....	16
2.2 Metal Head Gaskets.....	17
2.3 Copper Head Gaskets.....	19
2.4 O-rings.....	20
2.4.1 Measurement of Load Characteristics of the O-ring.....	22
2.5 Comparison of Gasket Types .....	24
<b>Chapter 3: Selection of Appropriate Solution</b> .....	<b>25</b>
3.1 Calculation of Screws .....	25
3.2 Design of Gaskets.....	32
3.2.1 Variant A .....	33
3.2.2 Variant B1 .....	34
3.2.3 Variant B2 .....	35
<b>Chapter 4: FEM Calculations</b> .....	<b>36</b>
4.1 Gasket Analysis Using Finite Element Methods .....	36
4.2 Process of Creating a Computational Model.....	36
4.3 Finite Element Model.....	37
4.4 Calculation Settings.....	44
4.5 Contacts Between Parts.....	48
4.6 Thermal Field of the Engine .....	53
4.6.1 Thermal Resistances .....	55
4.6.2 O-ring Temperatures .....	56
4.6.3 Cylinder Liner Temperatures .....	58
4.7 Effect of Combustion Pressure .....	61
4.7.1 Leakage Check of the O-ring for the Combustion Chamber.....	62
4.8 Stress of the Upper Mounting of the Cylinder .....	63
4.8.1 Stress of the Cylinder Head .....	63
4.8.2 Stress of the Cylinder Liner .....	66
4.8.3 Stress of the Copper Gasket .....	70
4.8.4 Stress of the Engine Block.....	71

4.9 FEMFAT Safety Calculations.....	72
4.9.1 Safety Factor of the Screw .....	73
4.9.2 Safety Factor of the Cylinder Liner .....	74
4.10 Cumulative Plastic Deformation of Engine Parts.....	76
4.10.1 Cumulative Plastic Deformation of the Cylinder Head.....	77
4.10.2 Cumulative Plastic Deformation of the Cylinder Liner .....	78
<b>Chapter 5: Conclusion .....</b>	<b>81</b>
<b>Cited Literature .....</b>	<b>83</b>
<b>List of Figures .....</b>	<b>84</b>
<b>List of Tables .....</b>	<b>86</b>
<b>List of Charts .....</b>	<b>87</b>
<b>List of Attachments .....</b>	<b>88</b>



## List of Symbols

$A_p$	surface of the cylinder base	$i$	number of threads
$C_1$	stiffness of the stressed part of the substitute tube	$k$	resulting dynamic safety factor
$C_2$	stiffness of the release part of the substitute tube	$k_{red\ max}$	maximum static stress safety factor
$C_s$	coefficient of the screw stiffness	$k_\sigma$	dynamic safety factor
$C_{Ta}$	stiffness of the stressed part of the connecting material	$k_\tau$	torsion safety factor
$C_{Tb}$	stiffness of the release part of the connecting material	$l_a$	stressed part of the substitute tube
$d$	width of the air layer	$l_b$	released part of the substitute tube
$D$	nut diameter of the substitute tube	$l_i$	length of the substitute tube
$d_1$	internal diameter of the O-ring	$M_k$	torsion of the screw when reaching the preload
$d_2$	thickness of the O-ring	$\dot{m}_{wb}$	water mass flow in the engine block
$D_2$	pitch diameter	$\dot{m}_{wh}$	water mass flow in the cylinder head
$d_3$	thread core diameter	$p$	maximum combustion pressure
$d'_3$	minimum thread core diameter	$P$	thread pitch
$d_v$	cylinder bore	$Q_0$	define preload
$E$	modulus of elasticity	$Q'_0$	minimal preload
$f$	friction coefficient - screw	$Q_{1a}$	amplitude force
$F$	force of four preload cylinder head screws	$Q_{1m}$	central operation force
$F_a$	force acting on the cylinder head by the combustion pressure	$q_z$	operating preload coefficient
$F_h$	force acting on the screw	$Q_z$	operating preload

R	thermal resistance	$\lambda$	thermal conductivity of the air
S	depth of the groove	$\rho_w$	density of water
$S'_3$	minimum cross-section of the thread core	$\mu$	coefficient of friction
$S_{Cu}$	copper gasket cross-section	$\nu$	utilization rate of the yield strength
$S_{EB-CL}$	surface of the contact engine block and cylinder liner	$\sigma$	stress
$S_i$	cross-section of the substitute tube	$\sigma_{1max}$	maximum tensile stress
$S_T$	surface of the nut	$\sigma_a$	tensile stress from amplitude force
T	temperature	$\sigma_{Cu}$	contact pressure between the copper gasket and the cylinder head
$\dot{V}_{wb}$	water flow rate in the engine block	$\sigma_{c(-1)}$	fatigue limit for the pulsating stress
$\dot{V}_{wh}$	water flow rate in the cylinder head	$\sigma_{EB-CL}$	contact pressure between the engine block and the cylinder liner
$W_k$	torsional section modulus	$\sigma_m$	tensile stress from central operating force
$\alpha$	thermal expansion coefficient	$\sigma_{pt}$	tensile strength
$\beta$	thread angle	$\sigma_{red max}$	maximum reduced stress
$\beta_n$	flank angle profile	$\sigma_{Q_0}$	tensile stress from preload
$\gamma$	thread pitch angle	$\sigma_{KT}$	yield strength
$\varepsilon$	strain	$\tau$	torsional stress.
$\phi$	overall reduction in the fatigue strength coefficient	$\tau_k$	maximum permitted torsion
$\kappa_\chi$	coefficient of influence of torsion	$\Psi_\sigma^x$	influence factor of the $\sigma_m$

## List of Abbreviations

ZK	cylinder head
ZKG	engine block
BUCHSE	cylinder liner
ZKS_A	screws on the side of the exhaust valves
ZKS_E	screws on the side of the intake valves
O-RING GENERAL	general contact around the circumference of the O-ring
GA	copper gasket
VF_A	valve guides of the exhaust valves
VF_E	valve guides of the intake valves
SR_A1(2)_A	valve seats on the side of the exhaust valves – axial surface
SR_E1(2)_A	valve seats on the side of the intake valves – axial surface
SR_A1(2)_R	valve seats on the side of the exhaust valves – radial surface
SR_E1(2)_R	valve seats on the side of the intake valves – radial surface
MPI	naturally aspirated engine
TSI	supercharged engine

# Chapter 1: Introduction

Internal combustion engines are continuously developed. Companies must satisfy customers who want higher power and lower fuel consumption. Companies must also take into account requirements for the reduction of pollutant emissions.

This work is part of a larger project that deals with the design of the new single-cylinder petrol engine that will be used in the laboratory. The engine will be used for many experimental measurements. The aim of this diploma thesis is to perform a literature search of contemporary cylinder head gasket designs, perform an assessment of the appropriate gasket design for a one cylinder research engine, perform mechanical stress calculations, perform thermal load calculations of the gasket and create manufacturing documentation of the cylinder head gasket and its assembly. Preliminary design of the geometry of the engine block and cylinder head was available at the beginning of this thesis. The engine block is designed as a closed deck. The thermal field of the cylinder head is available for the gasket design. The temperature, pressure and heat transfer coefficient in the cylinder versus crank angle graph are also available.

The cylinder head gasket must seal the combustion chamber and subsequently the space where the water flows. A wet cylinder liner will be used in this experimental engine. I will place demands on temperature resistance, resistance to combustion pressure, chemical resistance and also manufacturing and affordability.

It must be taken into account that the engine will only work in laboratory conditions and due to the various measurements and testing the engine will often be disassembled.

All calculations will be performed with the boundary conditions for both the naturally aspirated engine and the supercharged variant.

## 1.1 Experimental Single-Cylinder Engine

This is a four stroke experimental petrol engine. The engine displacement of this single-cylinder petrol engine is 374,5 cc. Stroke is 84,9 mm and bore is 74,5 mm. The engine has to be dimensioned for the maximum combustion pressure of 130 bar and a maximum speed of 7000 rpm.

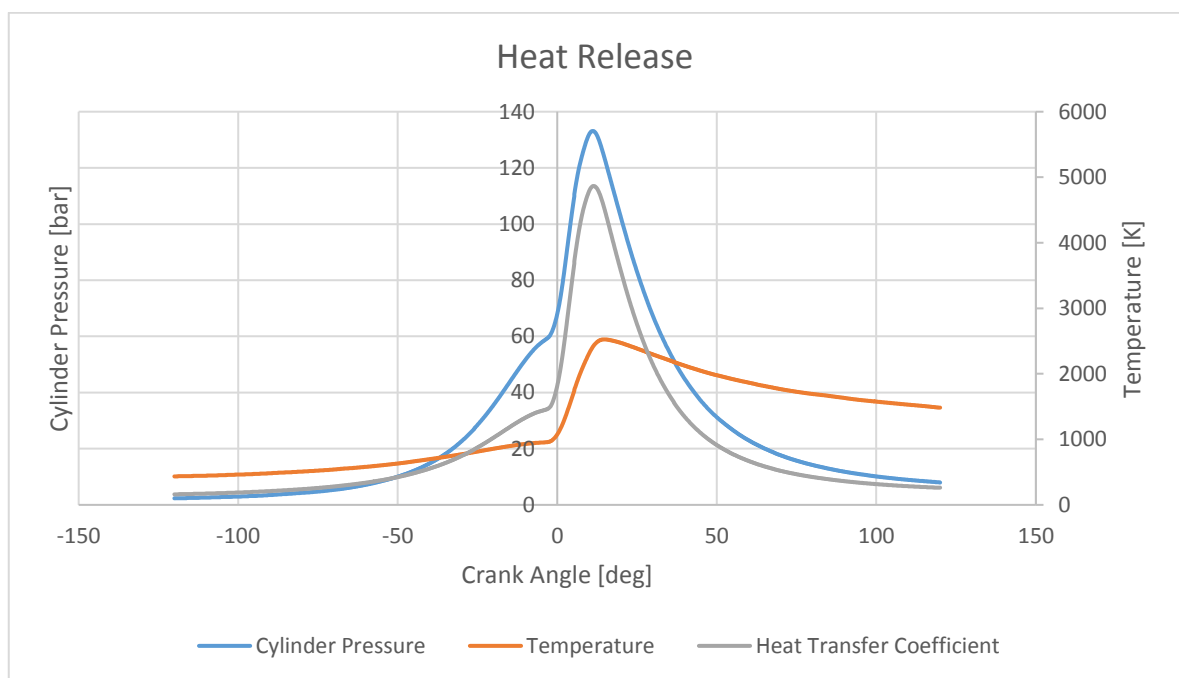
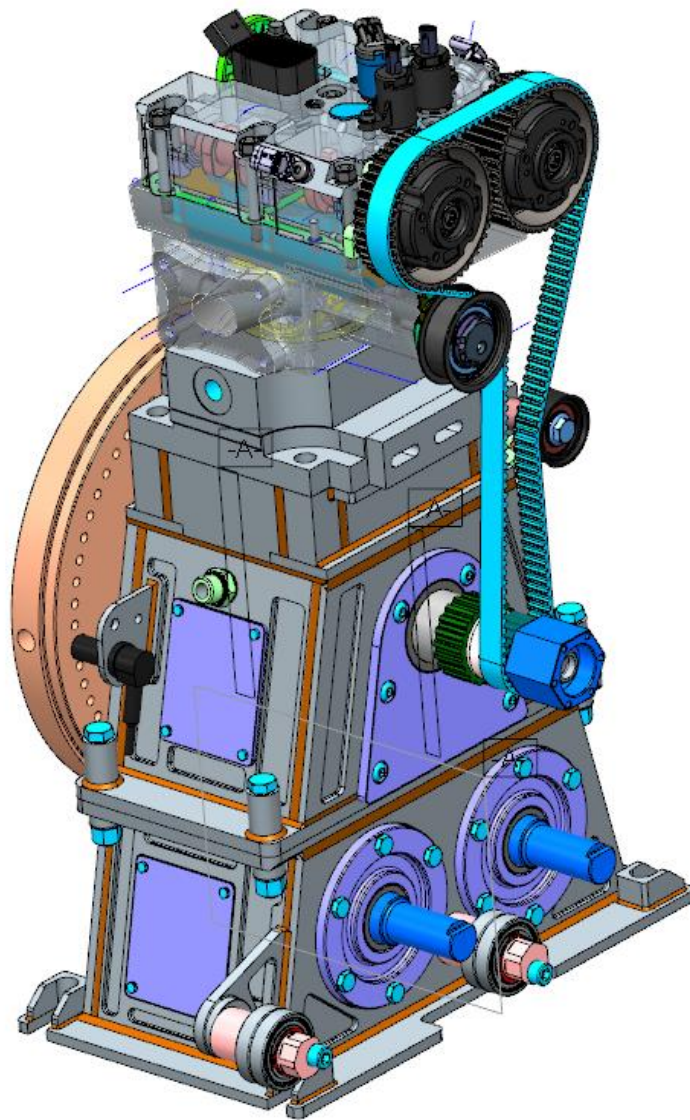


Chart 1: Heat Release

The maximum temperature of the ignited mixture in the cylinder is calculated at 2 525 K. Chart 1 shows the dependence of the temperature, pressure and heat coefficient on the crank angle. The peak of the combustion pressure is 11 degrees behind the top dead center. This engine has a wet cylinder liner. We must take into account the sealing of the combustion chamber and the water.

The engine will be used in the laboratory. The lowest ambient temperature will therefore be around 20 °C.



*Figure 1: Engine Model*

The engine is composed of four basic construction units (see Figure 1). At the bottom is the lower casing. Balance shafts are placed at the lower casing and the casing is provided with holes for mounting the engine to the pad. The engine has two counter-rotating balance shafts for balancing the sliding masses of the first order. The lower casing is bolted to the crankcase. The crankcase is inserted and bolted to the engine block. The engine block is bolted to the cylinder head with a valve cover. The water and oil system is also designed as an external drive independent of the combustion engine running.

We are most interested in the engine block and cylinder head in this diploma thesis because the cylinder head gasket will be positioned directly between these parts.

## Chapter 2: Head Gaskets Basics

The cylinder head gasket is the most important passive sealing element in the internal combustion engine. It is positioned between the engine block and the cylinder head. The main purpose is to provide a gas tight seal between the cylinder, water jackets, oil passages and the ambient air, liquids and gases. It must be able to accomplish this at all engine temperatures and pressures without malfunction, as a failure of the engine gasket usually results in a failure of the full engine.

When choosing a suitable gasket, we need to compare the advantages and disadvantages of the composite gaskets, metal gaskets and Viton O-rings.

Figure 2 shows the design process of the cylinder head gasket.

[3]

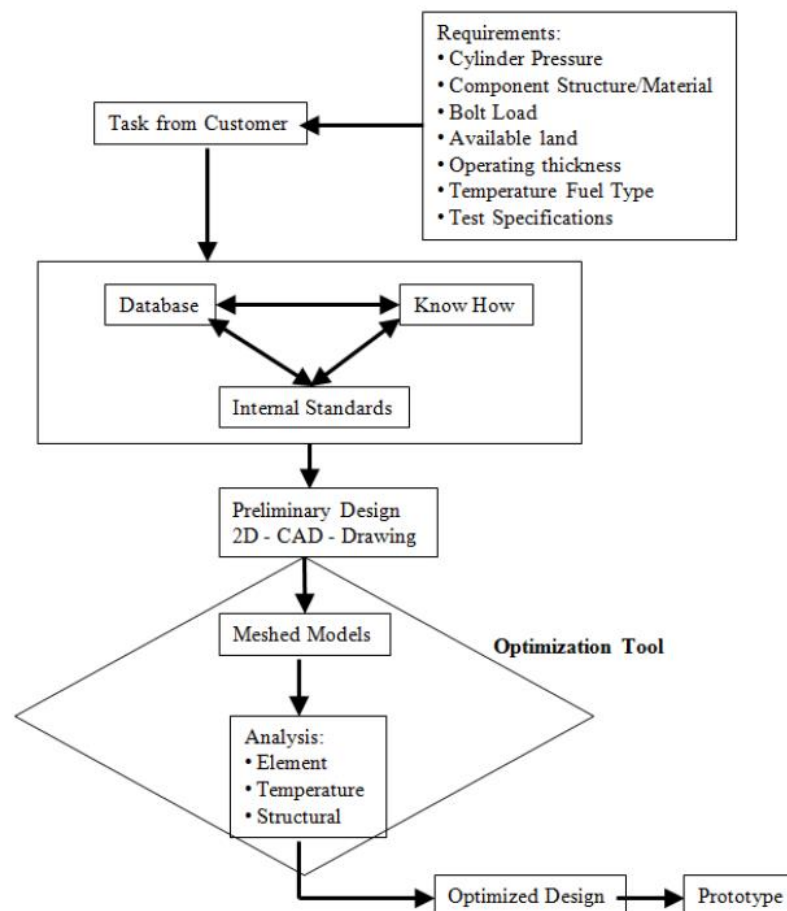


Figure 2: Design Process of the Gasket [3]

## 2.1 Composite Head Gaskets

### Types of composite head gaskets:

- a) Thin gasket sheeting bonded to a steel core with a fire ring at the cylinder bore and various kinds of coatings to seal fluids.
- b) Perforated metal with a compressible core such as flexible graphite, again with a coating for sealing and a fire ring around the bores.
- c) Perforated metal core with facing material such as flexible graphite mechanically clinched to the core and fire rings around the bores.

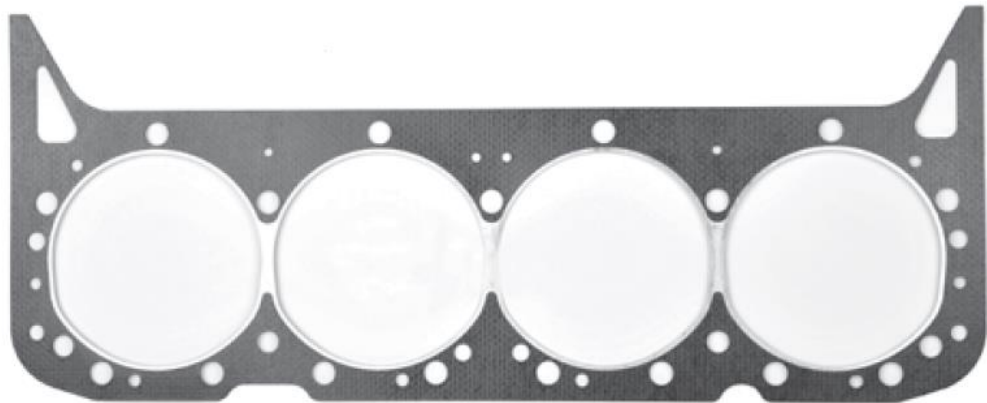


Figure 3: Composite Head Gasket [1]

The major differences are mentioned above. Composite gaskets do not require additional sealants. These types of gaskets are capable of sealing less than perfect surfaces due to the overall compressibility and capillary sealing qualities of the facing materials. Perforated metal with a compressible core and perforated metal core with facing material are simple, strong and have a good resistance to heat.

The disadvantages of this gasket are large deformations, which can affect the compression of the engine and when this overloads of the gasket can burn out. Nowadays it is used for repairing older engines.



## 2.2 Metal Head Gaskets

- a) Shim steel is the oldest of the pure metal gaskets. It is simple, thin and has stamping of a special alloy that is embossed around the openings to achieve a load differential. These head gaskets require the use of a sealant and are coated with special paint. O-rings are not used.
- b) MLS – multi layer steel is a relatively new method. The construction consists of two or more embossed stainless sheets riveted to a flat metal core. This method offers some advantages over the shim steel, they are available in different thicknesses so the designer can adjust compression height and they do not require additional sealant due to a micro thin layer of nitrile rubber or flour elastomer sealant applied to the facing. Due to the hardness of stainless steel MLS gaskets require a very smooth finish surface or leaks may result. This method is used for diesel and high power petrol engines with direct injection. It has good compensation of dynamics oscillation. The MLS head gasket can be used only once. After removing the cylinder head, it is necessary to place a new head gasket. Production of MLS head gaskets is expensive compared to other methods, because it is necessary to produce a tool for production first.

[1]

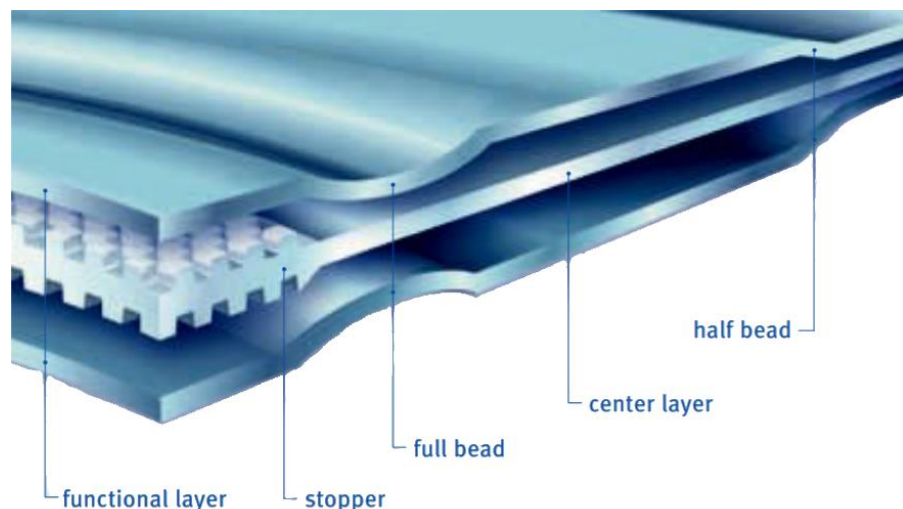


Figure 4: MLS Cross-section [4]

**Expertise in MLS gaskets, layer by layer:**

Half beads generate two-line compression. They seal along the water and engine oil passages, around the screw holes, and the circumference of the outer sealing contour.

Full beads generate three-line compression around the circumference of the combustion chamber. This elastic sealing element enables the sealing of very high ignition pressures, even in the presence of large dynamic sealing gap oscillations.

Functional layers are elastomer-coated spring steel layers which are equipped with elastic beads.

Center layer function is to adapt the gasket thickness to the installation conditions required by the design.

The engine components are elastically prestressed by the stoppers around the circumference of the combustion chamber. This helps achieve a reduction in the sealing gap oscillations caused by the gas force, while simultaneously preventing an impermissible deformation of the full beads.

[4]



Figure 5: MLS Head Gasket [13]

## 2.3 Copper Head Gaskets

Solid copper is capable of sealing more combustion pressure than shim steel or MLS head gaskets. It can be combined with an O-ring. Copper gaskets offer the most options to the engine designer for bore and thickness. Coolant leaks typically associated with copper gaskets are no longer an issue. Copper head gaskets can be reused several times as long as there are no signs of combustion leakage past the O-ring combustion seal. Leakage will be evidenced by carbon tracking beyond the combustion seal. Copper head gaskets are excellent heat conductors. It means that the block temperature and the cylinder head temperature will be more even.

[1]



*Figure 6: Copper Head Gasket [12]*

Copper is stronger than any composite head gasket yet still malleable so it conforms to the sealing surfaces. This strength-malleability combination is, more than any other attribute, the 'selling point' of copper as a head gasket material over other materials. The advantage of a malleable gasket is that conformity makes a tighter seal. It will show up in lower leak down percentages. This metal-to-metal solution does not require coating with additional sealants which have less resistance to heat or combustion pressure than metal.

The range of the thickness ranges from 0,5 mm to 2.4 mm.

[1]

## 2.4 O-rings

An O-ring is seal of rubber. The sealing ability is dependent on the O-ring, as well as the installation space. It depends on axial or radial compression of the O-ring cross-section. The O-ring is torus, i.e. a ring with a circular cross-section. It is made of synthetic rubber in precise dimensional tolerances and high surface quality. Installation space is mostly a groove against sealing surface. The rubber material acts as an incompressible highly viscous liquid with high surface tension. The pressure applied and storage leads to positive changes in the cross-section of the O-ring. The contact surfaces between the O-ring and installation space is an incremental preload acting of operating pressure.

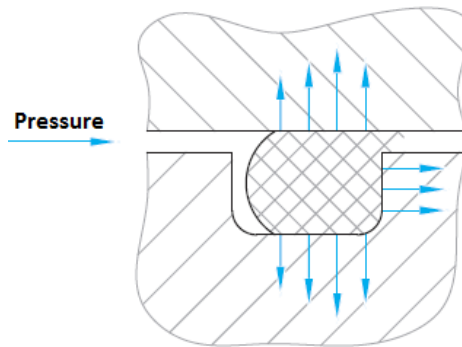


Figure 7: Acting of Operating Pressure [2]

O-rings can seal in a wide range of pressures, temperatures and tolerances. O-rings have easy maintenance and do not require tightening. They have small space requirements and low weight. Multiple use is possible unlike non-elastic gaskets. The lifetime, if properly matching the design, is of the normal period of aging rubber. O-ring failure usually manifests itself slowly and points to the need of replacement. It is the most economically advantageous design solution.

The dimension of the O-ring is indicated as the internal diameter times the cross-sectional diameter (thickness) of the ring –  $d_1 \times d_2$ .

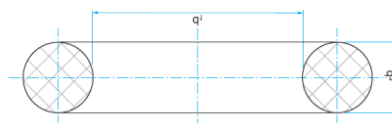


Figure 8: Dimensions of the O-ring [2]

For most applications, the newly proposed rectangular groove is preferred. In case supporting rings are not used, the bevel enabled hips 5°. If the supporting rings are used for reducing the leakage, the bevel side is of course not enabled.

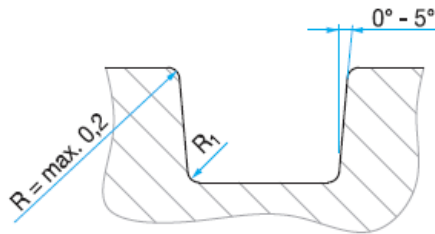


Figure 9: Rectangular Groove [2]

[2]

In cases where a groove cannot be used, it is possible to use a triangular installation space instead. The O-ring in this mounting space is seated in three sides.

[8]

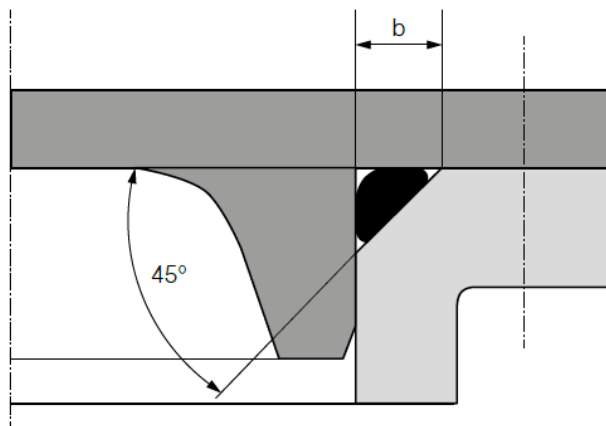


Figure 10: Triangular Installation Space [8]

Table 1: Operating Temperatures of the O-ring Materials [6]

Trade Name of the O-ring	Range of Operating Temperatures
Perbunan/Euoprene/Breon	-30°C ÷ 100°C
Viton/Fluorel	-20°C ÷ 250°C
Dutral/Buna EP	-45°C ÷ 110°C

Table 1 shows the operating temperatures of standard O-ring materials.

### 2.4.1 Measurement of Load Characteristics of the O-ring

Measurement of load characteristics were not used in the calculation, but served as an informative supplement only. The O-ring was ordered at Rubena a.s. It is a O-ring with the trade name Viton. The O-ring with a thickness of 2mm was tested.

The Zwick/Roell static material testing machine was used in ŠKODA-AUTO labs to measure the load characteristics of the O-ring. This machine can make the biggest force 5 kN.

The force measuring sensor Xforce was also Zwick/Roell and can measure up to 5 kN.

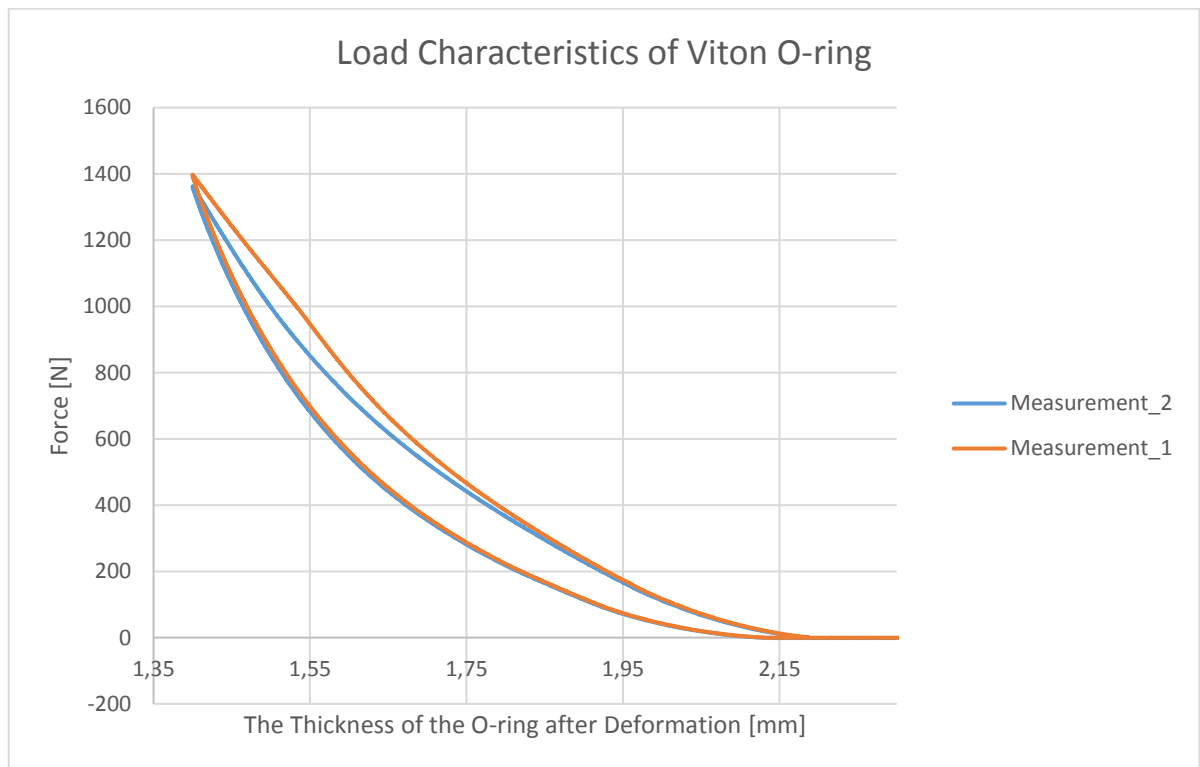


Chart 2: Load Characteristics of Viton O-ring

This Chart 2 shows that there is some hysteresis between the measurements.

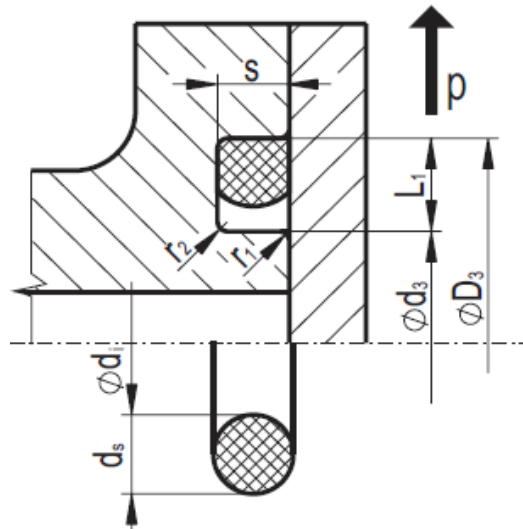


Figure 11: Axial Compression [6]

It is necessary to take into account tolerances in the depth of the groove  $S$  in the calculations. Groove depth tolerance using an O-ring with a diameter  $d_s$  up to 4 mm is 0,05/0 mm. We must consider as little pressure as possible on the O-ring on the wall. The groove depth  $S = 1,5$  mm. The biggest possible depth of the groove after adding the tolerance is 1,55 mm.

The lowest compressive force in this case may be 848 N.

## 2.5 Comparison of Gasket Types

Table 2: Comparison of Gasket Types

	<b>Composite Head Gaskets</b>	<b>Metal Head Gaskets</b>	<b>Copper Head Gaskets</b>	<b>O-rings</b>
<b>Advantages</b>	<ul style="list-style-type: none"> <li>• sealing less than perfect surfaces</li> <li>• strength and good resistance to heat</li> </ul>	<ul style="list-style-type: none"> <li>• available in different thicknesses</li> <li>• good compensation of dynamics oscillation</li> <li>• seals high pressures</li> <li>• resistant to high temperatures</li> </ul>	<ul style="list-style-type: none"> <li>• seals high pressures</li> <li>• most options to the engine designer for bore and thickness</li> <li>• excellent heat conduction</li> </ul>	<ul style="list-style-type: none"> <li>• seals high pressures</li> <li>• the most economical solution</li> <li>• can be used repeatedly</li> </ul>
<b>Disadvantages</b>	<ul style="list-style-type: none"> <li>• large deformations</li> <li>• when it overloads the gasket can burn out</li> <li>• necessary replacement after the engine head is disassembled</li> </ul>	<ul style="list-style-type: none"> <li>• MLS head gaskets are expensive compared to others methods</li> <li>• necessary to produce a tool for production</li> <li>• necessary replacement after the engine head is disassembled</li> </ul>	<ul style="list-style-type: none"> <li>• necessary replacement after disassembling of the engine head</li> </ul>	<ul style="list-style-type: none"> <li>• resistant to temperatures up to 250 °</li> </ul>



## Chapter 3: Selection of Appropriate Solution

Suitable type of head gasket must be selected with regard to the type of engine, production possibilities of the head gasket, cost and reliability. It is necessary to know the cylinder pressure, component structure/material, screw load, available land, operating thickness temperature fuel type and test specifications.

### 3.1 Calculation of Screws

We must take into account the highest pressure that may be present in the engine cylinder for the calculation of screws. In our case, we use the highest pressure of 130bar. This pressure in the cylinder causes force on the engine head. The surface of the engine head on which the combustion pressure acts can be derived from the surface of the cylinder base. The cylinder bore is 74,5 mm.

#### 1) Calculating the maximum force applied to the cylinder head:

$$A_p = \pi \times \frac{d_v^2}{4} = \pi \times \frac{74,5^2}{4} = 4\,359 \text{ [mm}^2\text{]} \quad (3.1)$$

$A_p$  [mm<sup>2</sup>] is the surface of the cylinder base and the  $d_v$  [mm] is the cylinder bore. Force  $F_a$  [N] acting on the cylinder head is derived from the formula below, where  $p$  [MPa] is the maximum combustion pressure.

$$F_a = A_p \times p = 4\,359 \times 13 = 56\,667 \text{ [N]} \quad (3.2)$$

This single cylinder engine has four cylinder head screws.  $F_h$  [N] is the force acting on one cylinder head screw.

$$F_h = \frac{F_a}{4} = \frac{56\,667}{4} = 14\,166 \text{ [N]} \quad (3.3)$$

## 2) Preliminary thread calculation, screw design and substitute tube design

The value of the operating preload coefficient  $q_z$  [-] was selected.  $Q_z$  [N] is the operating preload.

$$q_z = \frac{Q_z}{F_h} = 1,3 \quad (3.4)$$

The minimum cross-section  $S'_3$  [ $mm^2$ ] of the thread core is determined from the formula below, where the  $v$  [-] is the utilization rate of the yield strength,  $\sigma_{KT}$  [ $N \cdot mm^{-2}$ ] is the yield strength and  $\kappa_\chi$  [-] is the coefficient of influence of torsion.  $d'_3$  [mm] is the minimum thread core diameter.

$$\frac{F_h}{S'_3} \leq \frac{v \cdot \sigma_{KT}}{\kappa_\chi \cdot (1 + q_z)} \quad (3.5)$$

$$S'_3 = \frac{\pi \cdot d'^3_3}{4} [mm^2] \quad (3.6)$$

The screws in the cylinder head in the proposed single cylinder engine have a metric thread M9. The strength class of these screws is 12.9. The tensile strength of this strength class is 1 200 MPa and yield strength is 1 080 Mpa. The thread core diameter  $d_3 = 7,466$ .

$$d'_3 = \sqrt{\frac{4 \cdot F_h \cdot \kappa_\chi \cdot (1 + q_z)}{\pi \cdot v \cdot \sigma_{KT}}} = \sqrt{\frac{4 \cdot 14\,166 \cdot 1,2 \cdot (1 + 1,3)}{\pi \cdot 0,85 \cdot 1\,080}} \quad (3.7)$$

$$d'_3 = 7,36 [mm]$$

I chose screws M9x1,25 strength class 12.9.  $S_3$  [ $mm^2$ ] is the cross-section of the thread core and  $d_3$  [mm] is the thread core diameter.

$$S_3 = \frac{\pi \cdot d_3^2}{4} = \frac{\pi \cdot 7,466^2}{4} = 43,8 [mm^2] \quad (3.8)$$

### 3) Calculation of stiffness constants

The stiffness constants of the screw, cylinder head and engine block are calculated based on the idea of a substitute tube.

$$C_s = \frac{E}{\sum \frac{l_i}{S_i}} = \frac{2,1 \cdot 10^5}{\frac{100}{52,6}} = 1,1 \cdot 10^5 [N \cdot mm^{-1}] \quad (3.9)$$

$C_s [N \cdot mm^{-1}]$  is the coefficient of the screw stiffness,  $E [N \cdot mm^{-2}]$  is the modulus of elasticity,  $l_i [mm]$  is length of the substitute tube and  $S_i [mm^2]$  is the cross-section of the substitute tube.

$$D = 2 \cdot D_2 = 2 \cdot 8,188 = 16,376 [mm] \quad (3.10)$$

$D [mm]$  is the nut diameter of the substitute tube and  $D_2 [mm]$  is the pitch diameter.  $S_T [mm^2]$  is the surface of the nut.  $l_a [mm]$  is the stressed part of the substitute tube and  $l_b [mm]$  is the released part of the substitute tube.

$$S_T = \frac{\pi}{4}(D^2 - D_2^2) = \frac{\pi}{4}(16,376^2 - 8,188^2) = 157,97 [mm^2] \quad (3.11)$$

$$C_{Ta} = \frac{E \cdot S_T}{l_a} = \frac{2,1 \cdot 10^5 \cdot 157,97}{10} = 33,17 [N \cdot mm^{-1}] \quad (3.12)$$

$$C_{Tb} = \frac{E \cdot S_T}{l_b} = \frac{2,1 \cdot 10^5 \cdot 157,97}{90} = 3,69 \cdot 10^5 [N \cdot mm^{-1}] \quad (3.13)$$

Stiffness of the stressed part of the substitute tube  $C_1 [N \cdot mm^{-1}]$  and stiffness of the release part of the substitute tube  $C_2 [N \cdot mm^{-1}]$  are determined from the formulas below.

$$\frac{1}{C_1} = \frac{1}{C_s} + 2 \frac{1}{C_{Ta}} \rightarrow C_1 = 1,03 \cdot 10^5 [N \cdot mm^{-1}] \quad (3.14)$$

$$C_2 = C_{Tb} = 3,69 \cdot 10^5 [N \cdot mm^{-1}] \quad (3.15)$$

#### 4) Calculation of the preload and operational stress of the screw

Mounting preload  $Q'_0$  [N], central operation force  $Q_{1m}$  [N] and amplitude force  $Q_{1a}$  [N] are determined from the formulas below.

$$Q'_0 = \left( q_z + \frac{C_2}{C_1 + C_2} \right) \cdot F_h = \left( 1,3 + \frac{3,69 \cdot 10^5}{1,03 \cdot 10^5 + 3,69 \cdot 10^5} \right) \cdot 14\,166 \quad (3.16)$$

$$Q'_0 = 29\,490,5 \text{ [N]}$$

I define preload  $Q_0 = 31\,000$  [N].

$$Q_{1m} = Q_0 + \frac{1}{2} \cdot \frac{C_1}{C_1 + C_2} \cdot F_h = 31\,000 + \frac{1}{2} \cdot \frac{1,03 \cdot 10^5}{1,03 \cdot 10^5 + 3,69 \cdot 10^5} \cdot 14\,166 \quad (3.17)$$

$$Q_{1m} = 32\,546 \text{ [N]}$$

$$Q_{1a} = \frac{1}{2} \cdot \frac{C_1}{C_1 + C_2} \cdot F_h = \frac{1}{2} \cdot \frac{1,03 \cdot 10^5}{1,03 \cdot 10^5 + 3,69 \cdot 10^5} \cdot 14\,166 = 1\,545,7 \text{ [N]} \quad (3.18)$$

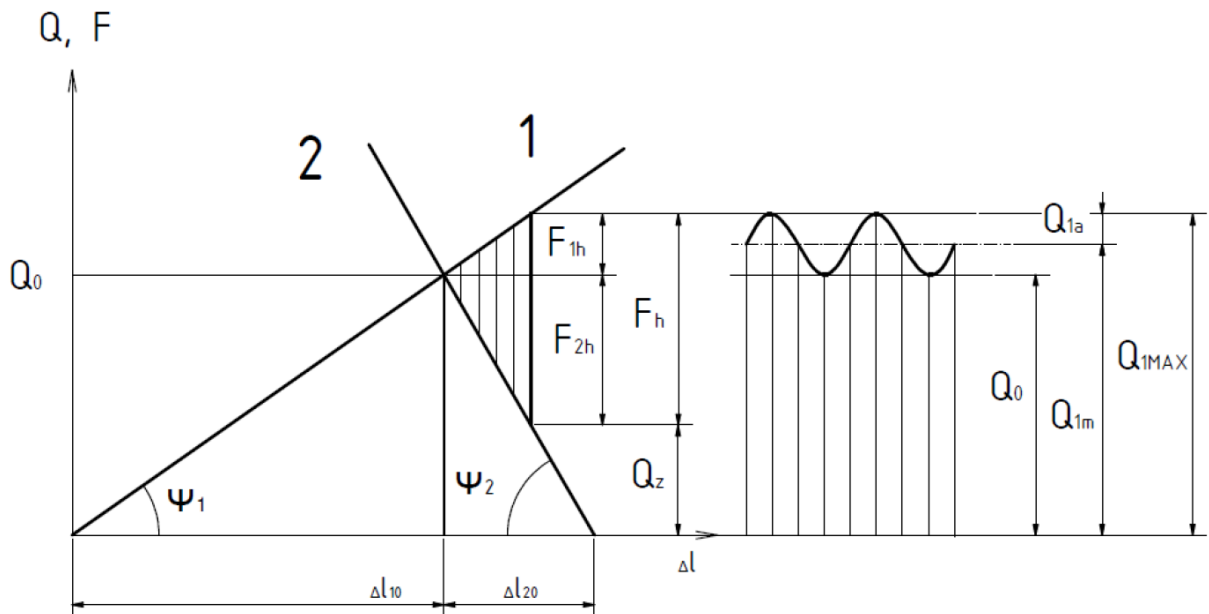


Figure 12: Mounting Preload [9]

$$\operatorname{tg} \psi_1 \cong C_1$$

$$\operatorname{tg} \psi_2 \cong C_2$$

Force magnitudes  $Q_0$ ,  $Q_{1m}$  and  $Q_{1a}$  correspond to the stress in the thread core.  $\sigma_{Q_0}$  [ $N \cdot mm^{-2}$ ] is the tensile stress from preload,  $\sigma_m$  [ $N \cdot mm^{-2}$ ] is the tensile stress from the central operating force and  $\sigma_a$  [ $N \cdot mm^{-2}$ ] is the tensile stress from amplitude force.  $\sigma_{1max}$  [ $N \cdot mm^{-2}$ ] is the maximum tensile stress.

$$\sigma_{Q_0} = \frac{Q_0}{S_3} = \frac{31\,000}{43,8} = 708 \text{ [N} \cdot \text{mm}^{-2}] \quad (3.19)$$

$$\sigma_m = \frac{Q_{1m}}{S_3} = \frac{32\,546}{43,8} = 743 \text{ [N} \cdot \text{mm}^{-2}] \quad (3.20)$$

$$\sigma_a = \frac{Q_{1a}}{S_3} = \frac{1\,545,7}{43,8} = 35,3 \text{ [N} \cdot \text{mm}^{-2}] \quad (3.21)$$

$$\sigma_{1max} = \sigma_m + \sigma_a = 743 + 35,3 = 778 \text{ [N} \cdot \text{mm}^{-2}] \quad (3.22)$$

Thread pitch angle  $\gamma$  [deg] is determined from the formula below where  $P$  [mm] is thread pitch and  $i$  [-] is number of threads.

$$\text{tg}(\gamma) = \frac{i \cdot P}{\pi \cdot d_2} = \frac{1 \cdot 1,25}{\pi \cdot 8,188} = 0,0486 \rightarrow \gamma = 2,782 \text{ [deg]} \quad (3.23)$$

Flank angle profile  $\beta_n$  [deg] is determined from the formula below where  $\beta$  [deg] is the thread angle and  $f$  [-] is the friction coefficient.

$$\begin{aligned} \text{tg} \beta_n &= \text{tg} \beta \cdot \cos \gamma = \text{tg} 30 \cdot \cos 2,782 = 0,577 \\ \text{tg} \beta_n &= 0,577 \rightarrow \beta_n = 29,98 \text{ [deg]} \end{aligned} \quad (3.24)$$

$$\text{tg} \varphi' = \frac{f}{\cos \beta_n} = \frac{0,15}{\cos (29,98)} = 0,173 \rightarrow \varphi' = 9,82 \quad (3.25)$$

$$\text{tg} (\gamma + \varphi') = \text{tg} (2,782 + 9,82) = 0,22 \quad (3.26)$$

### 5) Determination of fatigue strength characteristics and safety calculation

Torsion of the screw when reaching the preload  $M_k$  [ $N \cdot mm$ ] is determined below.

$W_k$  [ $mm^3$ ] is the torsional section modulus and  $\tau$  [ $N \cdot mm^{-2}$ ] is the torsional stress.

$$M_k = Q_0 \frac{d_2}{2} \cdot tg(\gamma + \varphi') = 31\,000 \cdot \frac{8,188}{2} \cdot 0,22 \quad (3.27)$$

$$M_k = 27\,921 \text{ [N} \cdot \text{mm]}$$

$$W_k = \frac{\pi \cdot d_3^3}{16} = \frac{\pi \cdot 7,466^3}{16} = 81,7 \text{ [mm}^3\text{]} \quad (3.28)$$

$$\tau = \frac{M_k}{W_k} = \frac{26\,561,5}{81,7} = 342 \text{ [N} \cdot \text{mm}^{-2}\text{]} \quad (3.29)$$

Torsion safety factor  $k_\tau$  [-] is calculated by HMM hypothesis.  $\tau_k$  [ $N \cdot mm^{-2}$ ] is the maximum permitted torsion.

$$\tau_k = 0,57 \cdot \sigma_{kt} = 0,57 \cdot 1080 = 615,6 \text{ [N} \cdot \text{mm}^{-2}\text{]} \quad (3.30)$$

$$k_\tau = \frac{\tau_k}{\tau} = \frac{615,6}{342} = 1,8 \quad (3.31)$$

Calculation of the maximum reduced stress  $\sigma_{red\,max}$  [ $N \cdot mm^{-2}$ ] for maximum operating load of the screw is determined in the formula below. HMM hypothesis is used.  $k_{red\,max}$  [-] is the maximum static stress safety factor.

$$\sigma_{red\,max} = \sqrt{\sigma_{1\,max}^2 + \alpha^2 \cdot \tau^2} = \sqrt{778^2 + \sqrt{3}^2 \cdot 342^2} \quad (3.32)$$

$$\sigma_{red\,max} = 978 \text{ [N} \cdot \text{mm}^{-2}\text{]}$$

$$k_{red\,max} = \frac{\sigma_{kt}}{\sigma_{red\,max}} = \frac{1\,080}{978} = 1,1 \quad (3.33)$$

$\sigma_{c(-1)}$  [ $N \cdot mm^{-2}$ ] is fatigue limit for the pulsating stress,  $\sigma_{pt}$  [ $N \cdot mm^{-2}$ ] is the tensile strength and  $\phi$  [-] is overall reduction in the fatigue strength coefficient.

$$\sigma_{c(-1)} = 0,61 \cdot \sigma_{pt} = 0,61 \cdot 1\,200 = 732 \text{ [N} \cdot \text{mm}^{-2}] \quad (3.34)$$

$$\sigma_{c(-1)}^x = \frac{\sigma_{c(-1)}}{\phi} = \frac{732}{5} = 146,4 \text{ [N} \cdot \text{mm}^{-2}] \quad (3.35)$$

The influence factor of the  $\sigma_m$  is the  $\psi_\sigma^x$  [-].  $k_\sigma$  [-] is the dynamic safety coefficient and  $k$  [-] is the resulting dynamic safety factor.

$$\psi_\sigma = 0,02 + 2 \cdot \sigma_{pt} \cdot 10^{-4} = 0,26 \quad (3.36)$$

$$\psi_\sigma^x = \frac{\psi_\sigma}{\phi} = 0,052 \quad (3.37)$$

$$k_\sigma = \frac{\sigma_{c(-1)}^x - \psi_\sigma^x \cdot \sigma_{Q_0}}{\sigma_a + \psi_\sigma^x (\sigma_m - \sigma_{Q_0})} = \frac{146,4 - 0,052 \cdot 708}{35,3 + 0,052 \cdot (743 - 708)} = 2,95 \quad (3.38)$$

$$k = k_\sigma \cdot \sqrt{1 - \left(\frac{1}{k_\tau}\right)^2} = 2,95 \cdot \sqrt{1 - \left(\frac{1}{1,8}\right)^2} = 2,45 \quad (3.39)$$

[9]

This analytical calculation is complemented by FEMFAT material fatigue calculation. FEMFAT (Finite Element Method Fatigue) is the engineering software tool for fatigue life prediction. It is used to improve reliability and robustness of components in the automotive and machinery industry.

The lowest safety factors of the screws calculated by FEMFAT with supercharged (TSI) variants range from 2.35 to 2.87.

### 3.2 Design of Gaskets

The use of composite gaskets has been ruled out with regard to seal thickness, large deformation and the danger of burnout when overloaded. A multi-layer metal gasket is unsuitable for use in single-piece engine manufacturing. The main reason is the cost of production that pays only for serial applications. The copper ring is able to seal high pressures, is inexpensive, space-saving, but after the engine has been disassembled a new copper gasket has to be applied due to the plastic deformation of the ring.

For the above reasons, it was decided to use a Viton O-ring to seal the combustion and water space. The O-ring is the cheapest solution, can seal high pressures, can be used repeatedly and is space-saving.

In the event that an O-ring that seals the combustion chamber is stressed at a higher temperature than the material can handle, we use a variant where the combustion chamber is sealed by the copper gasket. The cylinder liner, which has a groove for O-ring, will be also in danger of the critical stress at the point of the groove.

In both cases, water is sealed with an O-ring that is located between the cylinder liner and the engine block in the triangular installation space.

The O-ring cannot be in the groove in the engine block and be pressed into it by the cylinder head. The main reason is that a gap between the engine block and the cylinder head must be avoided due to the prestress of the cylinder liner. It is not possible to reduce the gap between the engine block and the cylinder head because there would be a risk of contact between these parts, which is undesirable.

The O-ring cannot be in the groove in the vertical wall of the engine block and pressed inwards by the cylinder liner due to the lack of space for this solution.

Two O-rings are used in variant A and one O-ring in combination with a copper gasket are used in variants B1 and B2.



### 3.2.1 Variant A

The first O-ring that seals the combustion chamber sits in a groove which is milled into the cylinder liner. The O-ring is forced into the groove by the cylinder head. The second O-ring that seals water sits in the triangular installation space between the engine block and the cylinder liner.

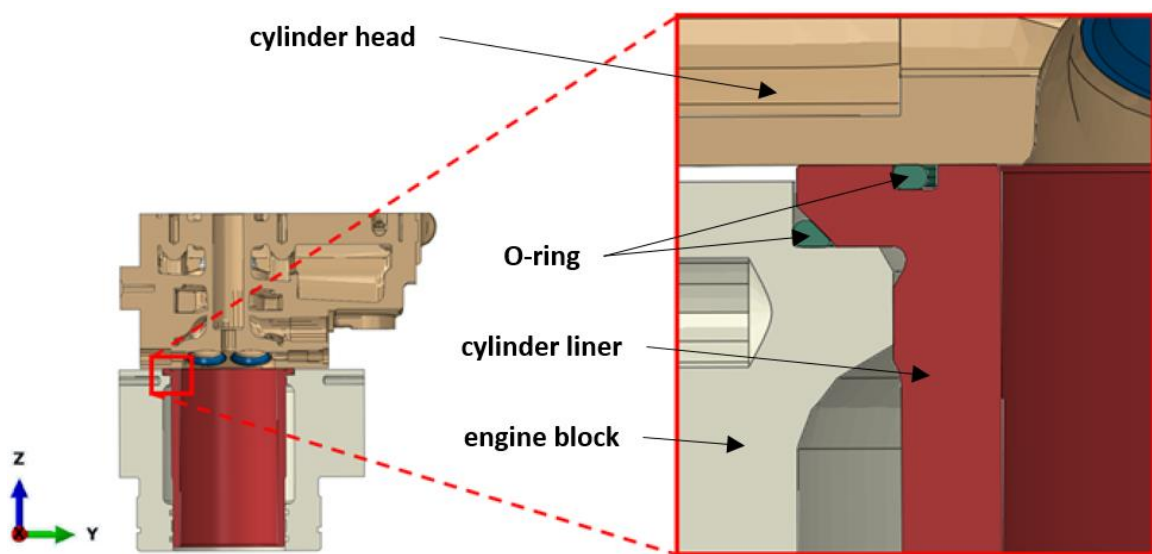


Figure 13: Variant A

#### Editing of geometry of engine parts – Variant A:

Due to the chamfering of the cylinder liner edge, the diameter of the top of the cylinder liner had to be increased to maintain the contact surface between the cylinder liner and engine block. The chamfering of the cylinder liner edge was required due to the location of the O-ring in the corner. Along with the cylinder liner, the hole in the engine block had to be extended also.

A groove was created in the cylinder liner for the second O-ring, which sealed the combustion chamber.

### 3.2.2 Variant B1

The O-ring that seals water sits in the triangular installation space between the engine block and the cylinder liner. The copper gasket that seals the combustion chamber sits between the cylinder liner and the engine head. The copper gasket is centered by the outer side of the cylinder liner.

If the copper gasket is centered from the inside, the edge of the cylinder liner may begin to overheat. This can cause engine knock. If the gasket is centered on the outside, this danger is avoided.

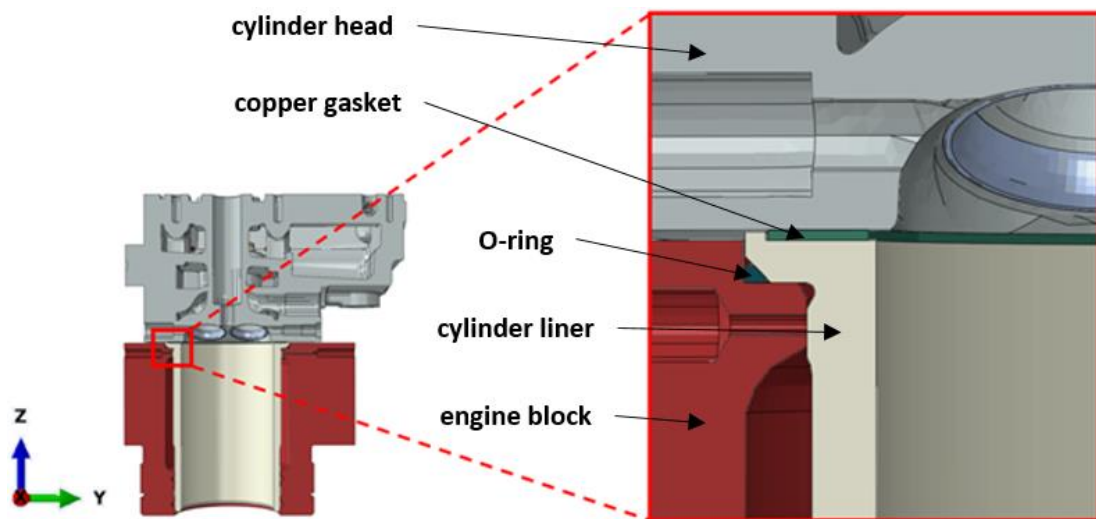


Figure 14: Variant B1

#### Editing of geometry of engine parts – Variant B1:

The engine block was modified as in variant A.

The cylinder liner also had a chamfer to install the O-ring in the corner. The raised edge on the outside is created by centering the copper gasket.

### 3.2.3 Variant B2

The O-ring that seals water sits in the triangular installation space between the engine block and the cylinder liner. The copper gasket that seals the combustion chamber sits between the cylinder liner and the engine head. The copper gasket is not centered.

This option would be inappropriate when used in serial production, but in the case of an experimental single-cylinder engine, this can be used, although it would need more care during assembly.

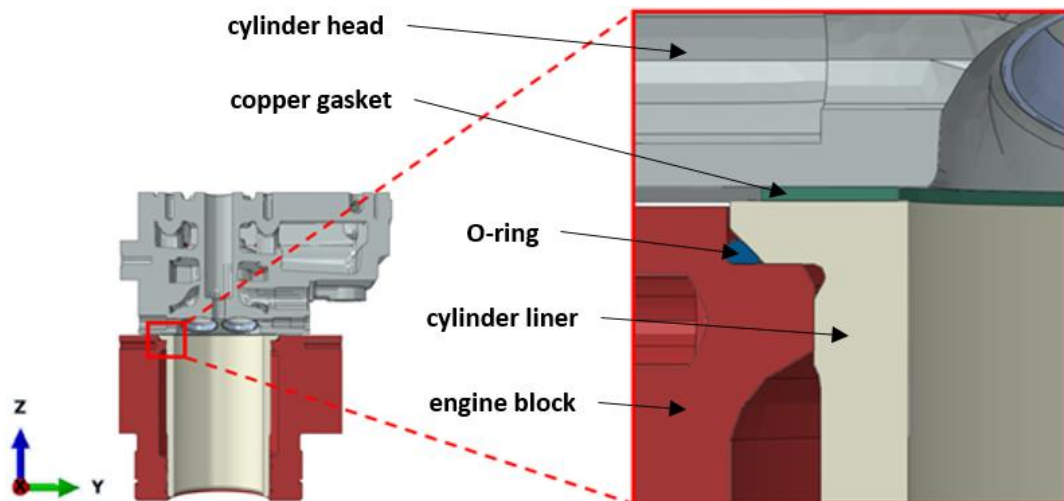


Figure 15: Variant B2

#### Editing of geometry of engine parts – Variant B2:

The engine block is modified as in variant A.

The surface of the top of the cylinder liner is straight, because the gasket is not centered in this variant.

All dimensions of engine parts modifications are in the technical documentation attached to this diploma thesis.

## Chapter 4: FEM Calculations

### 4.1 Gasket Analysis Using Finite Element Methods

Computer Aided Engineering (CAE) is an important tool for gasket design. It can reduce the time and costs of the engine development cycle. CAE can be used to make the first design proposal and first optimizations without using any hardware. The design process generally relies heavily on advanced experimental, analytical and numerical methods. It is very important to use the Finite Element method of the full engine assembly, including the gasket, in order to aid in the understanding of motion levels and deflections of the gasket sealing features, well before production. The pre-production analyses help the designer to understand the capability of the design to meet the sealing and durability requirements of the gasket while allowing it to be brought into production faster. The numerical simulation modeling allows the engineer to review multiple loading and operating conditions, which increase the probability of an initial design being successful.

The main approach to the finite element method involves modeling any structure with small, interconnected elements called finite elements. The displacement function is associated with each finite element. All of the finite elements are directly or indirectly linked to every other element. It is possible to determine the behavior at any node in the structure with regards to the properties of all other elements of the structure by applying the stress/strain properties of the material.

[3]

### 4.2 Process of Creating a Computational Model

Modifying the geometry of the engine block and the cylinder liner was necessary after selecting the appropriate sealing variants. Only preliminary designs of these engine parts were available at the beginning of the project. CAD data editing was done in CREO PARAMETRIC 2.0.

The advanced CAE pre-processing software ANSA served to prepare the calculation model. All CAD data of the entire model were imported into the ANSA program. When importing models, there were some geometry errors that needed to be corrected. The surface mesh was formed on the models after repairs and checking of all surfaces. The individual parts were positioned in the assembly. The properties of all contacts between the components were set. Each part was defined by material properties. The entire calculation was divided into individual steps describing the progress of the calculation from assembly, over the engine operating cycle and cooling down after the engine was switched off. The initial boundary condition of the motor temperature was set at room temperature of 20 °C. The temperatures of each model node were mapped during the calculation after the engine was assembled. The pressure in the combustion chamber was set in the next step after the engine was warmed to the operating temperature.

All sealing variants were calculated for the boundary conditions that best describe the assembly and working cycle of the naturally aspirated engine as well as supercharged engine variant.

The post-processing results of the computational models were evaluated in the program Abaqus Viewer. Stresses, contact pressures, temperatures and deformations were investigated in this software.

### **4.3 Finite Element Model**

The finite Element Model in variant A consists of an engine block, a cylinder liner, two O-rings, an engine head, valve seats, valve guides and four head screws. Variants B1 and B2 have a copper gasket instead of one O-ring. Variants B1 and B2 also use another cylinder liner. Each of these parts was imported into the ANSA program in the IGES format. After importing each part into ANSA, geometry was checked and repaired because of an error in data transmission.

Mesh density and the number of elements in the whole set are also computed with respect to computational capacities.

The engine block is discretized by 80 394 volume elements. The type of the volume elements is quadratic tetra C3D10. It is called the ZKG in the computational model. The mesh is much finer inside the block, near the combustion chamber, than the outside; therefore a much more accurate calculation is needed in this place. Higher stress is expected in the inside because of the higher temperatures and the cylinder liner which is pressed to the engine block.

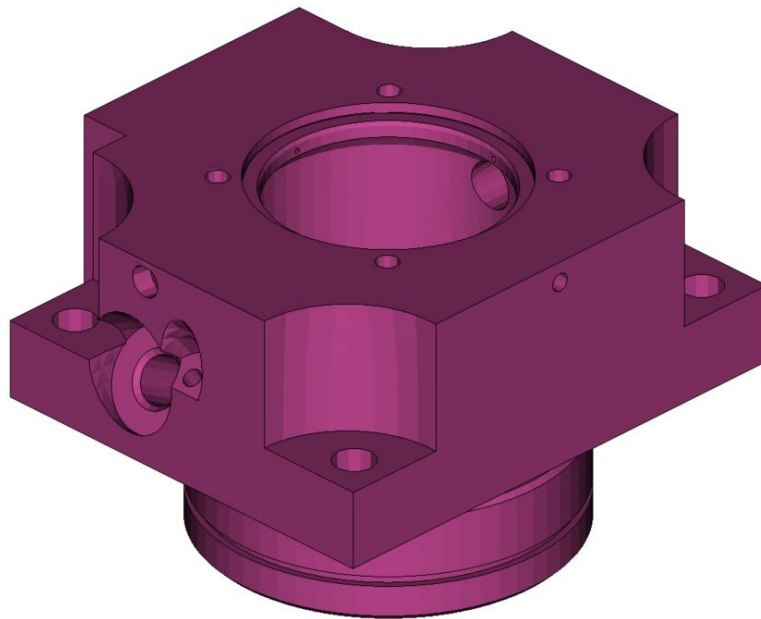


*Figure 16: Engine Block*

The engine block is manufactured by machining a steel cube. The standard of this steel is ČSN 11 500. The engine block material was described by modulus of elasticity, Poisson constant and expansion coefficient.

The cylinder head is discretized by 372 709 volume elements. The type of the volume elements is quadratic tetra C3D10. It is called the ZK in the computational model. The much finer mesh was created at the surface which is in the contact with the cylinder liner, in the holes for the screws and the valve guides and also at the surface where the valve seats fit. The cylinder head is made from aluminium alloy AlSi10Mg.

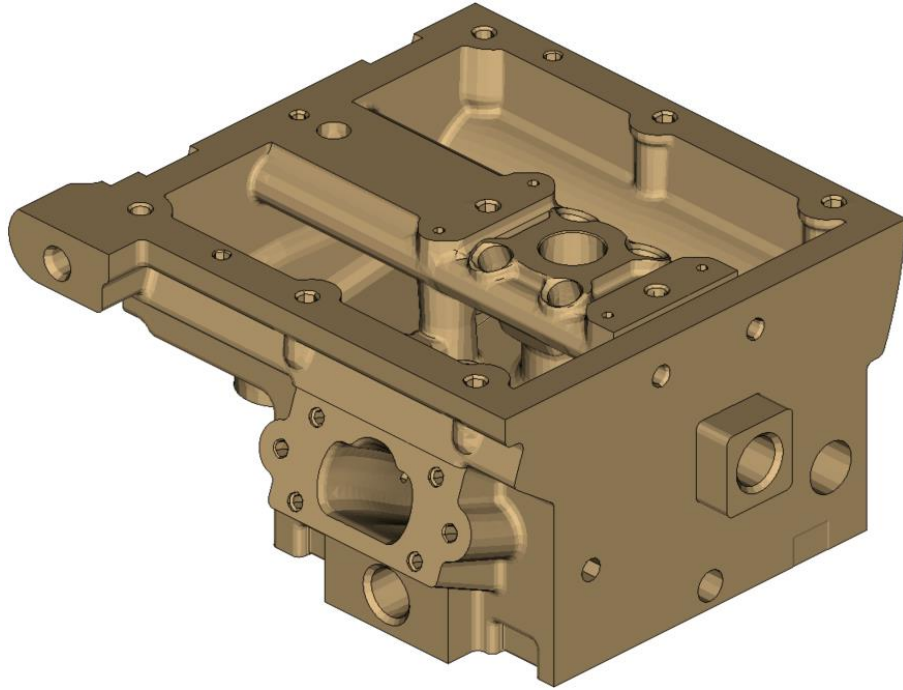


Figure 17: Cylinder Head

Chart 3 shows a Stress-strain diagram of the AlSi10Mg for different temperatures.

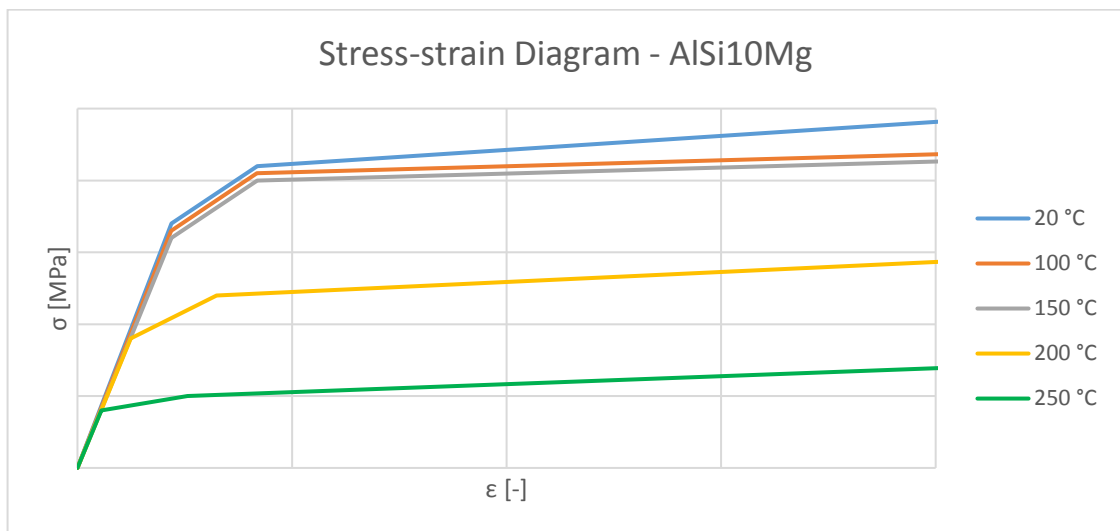


Chart 3: Stress-strain Diagram of the AlSi10Mg

The O-rings are discretized by 1 440 volume elements. The type of the volume elements is quadratic penta C3D15. The O-rings are made of material with the trade name Viton.

Viton is a brand of synthetic rubber and fluoropolymer elastomer. Viton has a hardness of 80 ShA and the heat resistance of this material ranges from -20 °C to 250 °C.

The O-ring material was described by modulus of elasticity, Poisson constant and expansion coefficient.

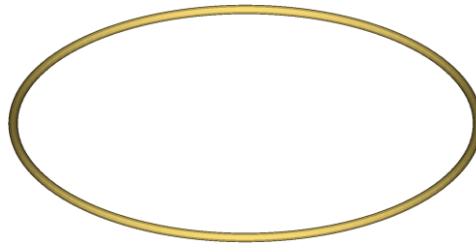


Figure 18: O-ring 96x2

The cylinder head screw is discretized by 2 929 volume elements. The type of the volume elements is quadratic tetra C3D10. It is called the Schrauben in the computational model. The cylinder head screw is made of heat treatment steel. Its material code is 30CrNiMo8. The screw strength class is 12.9. Four screws are used in the model.

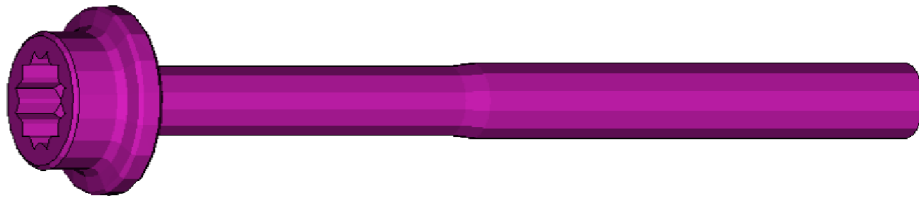


Figure 19: Screw M9x100

Chart 4 shows the dependence of the thermal expansion coefficient  $\alpha$  [ $\text{K}^{-1}$ ] of the material 30CrNiMo8 on the temperature  $T$  [ $^{\circ}\text{C}$ ].

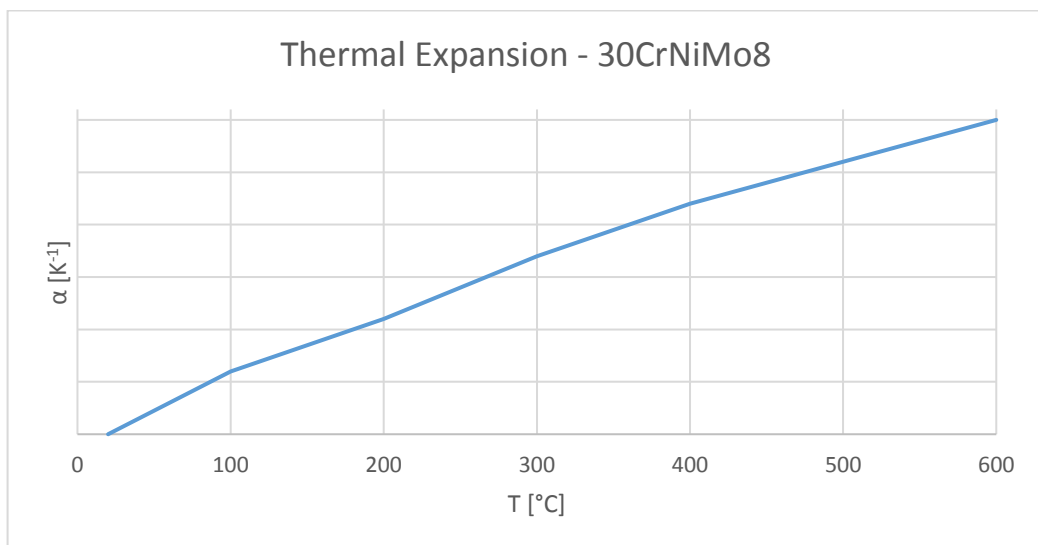


Chart 4: Thermal Expansion of the 30CrNiMo8



Chart 5 shows the dependence of the modulus of elasticity  $E$  [GPa] of the material 30CrNiMo8 on the temperature  $T$  [°C].

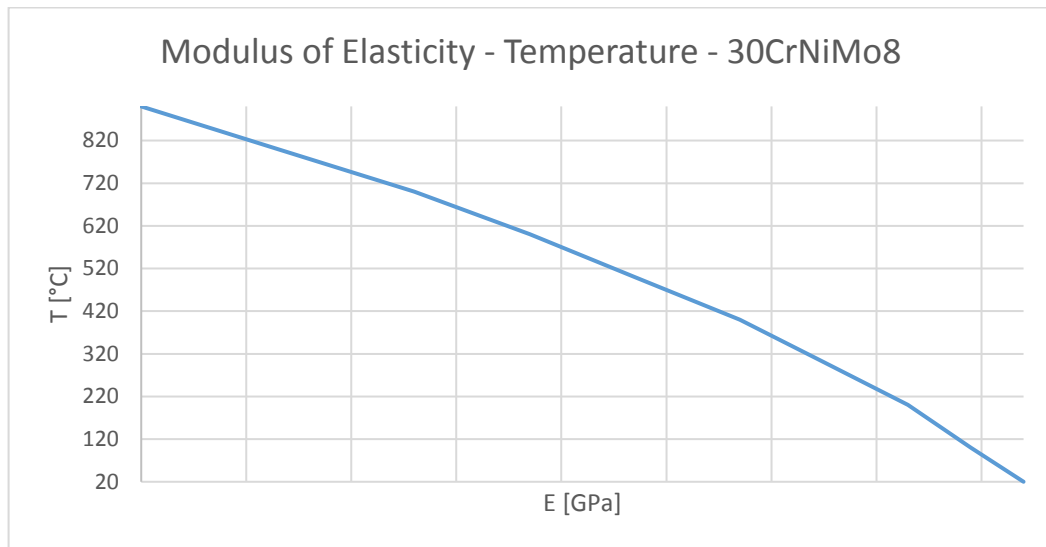


Chart 5: Modulus of Elasticity of the 30CrNiMo8

The intake valve seat is discretized by 480 volume elements. The exhaust valve seat is discretized by 360 volume elements. The type of the volume elements is quadratic hexa C3D20. It is called the SR\_A (exhaust) and SR\_E (intake) in the computational model. Two intake valve seats and two exhaust valve seats are used in the model. The valve seats material is the sintered steel. TL\_4791 is the internal name in Volkswagen.



Figure 20: Intake Valve Seat (left) and Exhaust Valve Seat

The cylinder liner variant A is discretized by 62 565 volume elements. The cylinder liner variant B1 has 74 004 volume elements and the cylinder liner variant B2 has 67 213 volume elements. The type of the volume elements is quadratic tetra C3D10. It is called the Buchse in the computational model. The cylinder liner is cast from the material EN-GJL-350. The yield strength of the material EN-GJL-350 is 228-285 MPa.

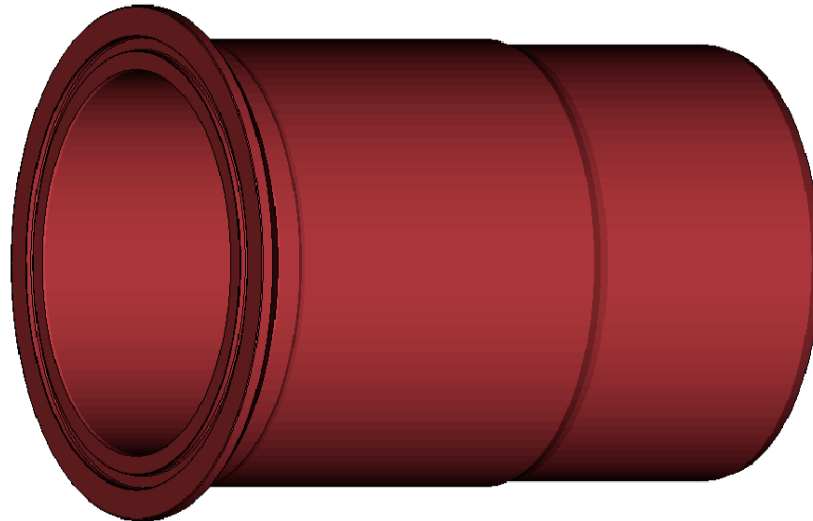


Figure 21: Cylinder Liner A

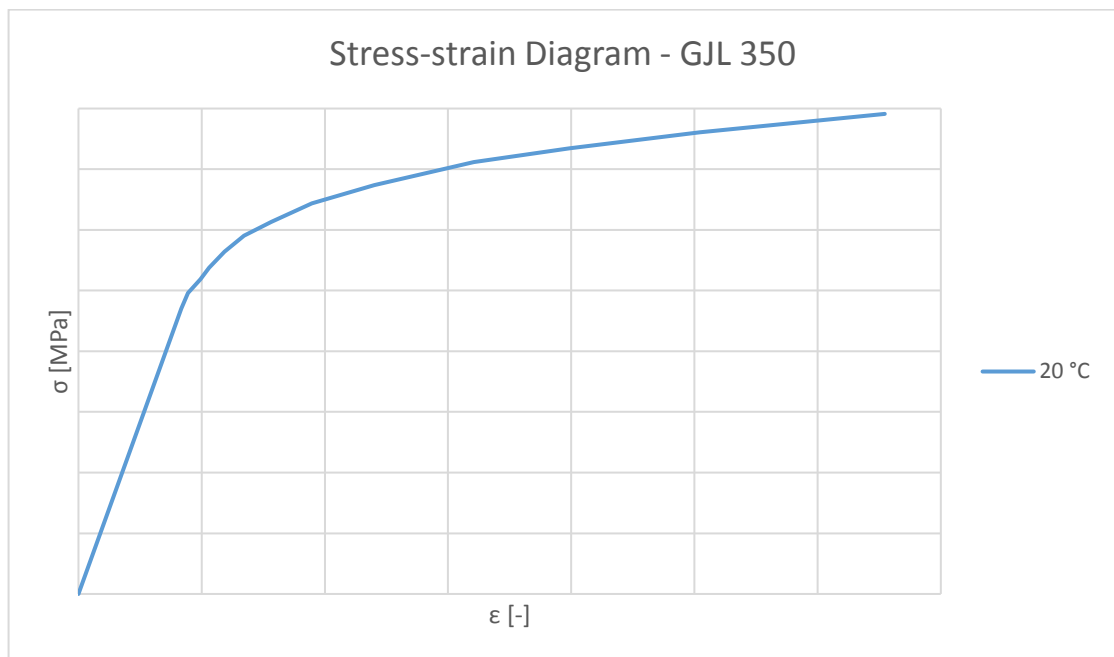


Chart 6: Stress-strain Diagram of the GJL 350.

Chart 6 shows Stress-strain diagram of the material GJL 350 at 20°C.

The intake valve guide is discretized by 4 149 volume elements and the exhaust valve guide is discretized by 4 357 volume elements. The type of the volume elements is quadratic tetra C3D10. It is called the VF\_A (exhaust) and VF\_E (intake) in the computational model.

The valve guides material is the sintered steel. TL\_4791 is the internal name in Volkswagen for material of exhaust valve guides. TL\_080 is the internal name in Volkswagen for material of intake valve guides.

Two intake valve guides and two exhaust valve guides are used in the model.



Figure 22: Intake Valve Guide (left) and Exhaust Valve Guide

The copper gasket is discretized by 3 687 volume elements. The type of the volume elements is quadratic tetra C3D10. It is called the GA in the computational model.

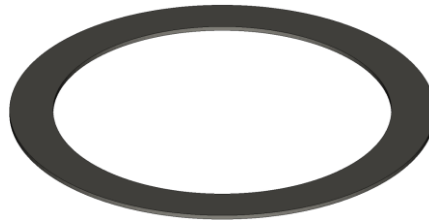


Figure 23: Copper Gasket

Table 3 describes how many and what type of volume elements the individual models have.

Table 3: Numbers and Types of Elements

	Number of Elements	Type of Volume Element
Engine Block	80 394	quadratic tetra C3D10
Cylinder Head	372 709	quadratic tetra C3D10
Cylinder Liner – A	62 565	quadratic tetra C3D10
Cylinder Liner – B1	74 004	quadratic tetra C3D10
Cylinder Liner – B2	67 213	quadratic tetra C3D10
O-ring Water	1 440	quadratic penta C3D15
O-ring Combustion	1 440	quadratic penta C3D15
Copper Gasket	3 687	quadratic tetra C3D10
Valve Seat Exhaust	360	quadratic hexa C3D20
Valve Seat Intake	480	quadratic hexa C3D20
Valve Guide Exhaust	4 357	quadratic tetra C3D10
Valve Guide Intake	4 149	quadratic tetra C3D10
Cylinder Head Screw	2 929	quadratic tetra C3D10

## 4.4 Calculation Settings

The entire calculation is divided into seven steps in all variants. These steps are pressing, tightening, fixing, heating, ignition, after ignition and cool engine to the room temperature.

### First computational step

Six degrees of freedom are removed from the engine block by using the boundary conditions. One degree of freedom in axial direction is removed from the engine block on the bottom surface which is supported to the crankcase. The second degree of freedom is removed in the axial direction from the surface to which the cylinder liner is pressed. The rest of the degrees of freedom were removed by fixing of the screw holes in the lower part of the engine block in the radial and tangential direction. The engine block is fixed by means of boundary conditions on the spot because it is bolted to the chassis. The degrees of freedom of the other components take the contacts listed in Table 5.

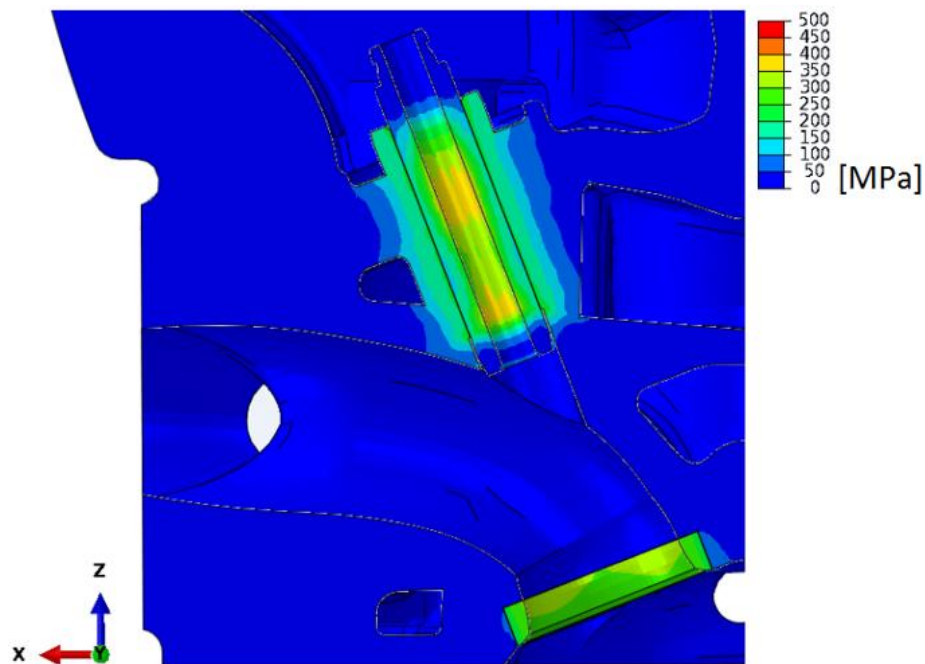


Figure 24: Valve Seats and Valve Guides Pressed into the Cylinder Head

The O-rings are pressed into the sealing area by a low force in the first step. This force is set to 310 N by tightening of the screws. Pressing the O-rings with less force in the first step is done because of better converge of the calculation. This is due to the fact that the O-ring has a much lower modulus of elasticity than the engine block, cylinder liner or cylinder head. The seat and valve guides are pressed into the cylinder head. The temperature of all parts is set to a room temperature 20 °C. The wall contacts between the cylinder liner and the engine block are interrupted due to moving these components during assembly. If these contacts were active during assembly, this could cause convergence problems.

### Second computational step

In the second step, the screws are tightened to the desired preload. The force applied by each screw to the cylinder head after tightening is 31 000 N (See Equation 3.16). All the parts are in the final positions after this step.

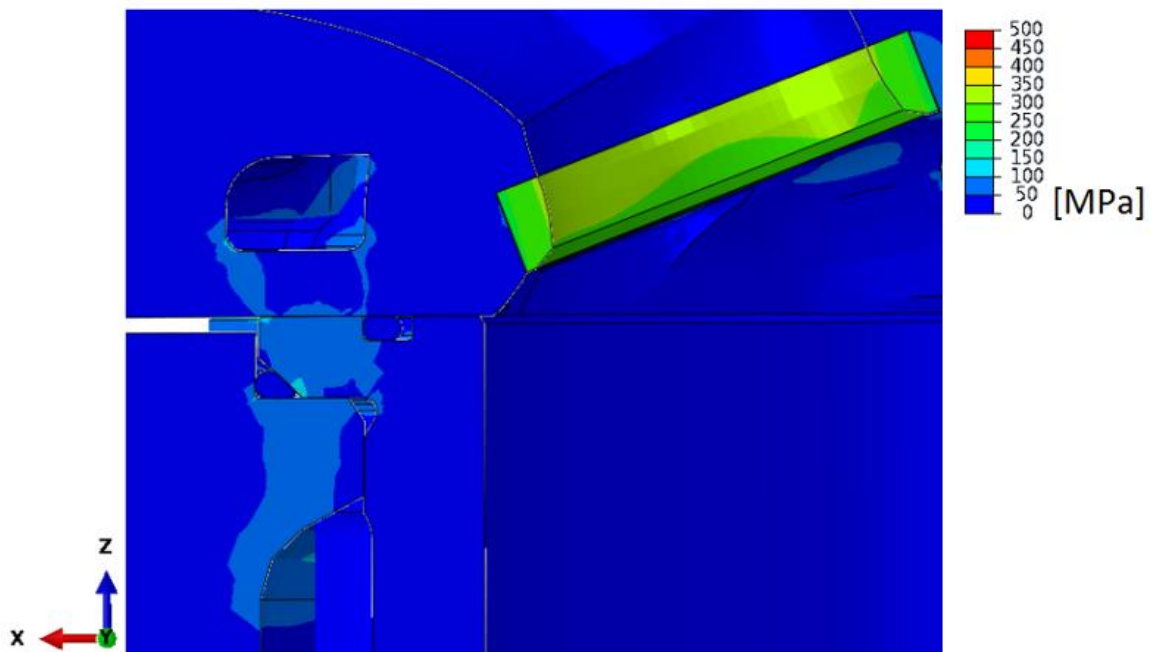


Figure 25: Stress after Tightening to the Desired Preload

### Third computational step

The setting of the third step holds the screws in place after tightening in place. This is the default state for the loading of the engine operating conditions. In this step the contacts between the cylinder liner and the engine block are turned on.

### Fourth computational step

Temperatures are mapped to individual nodes in the fourth step. The thermal field is described in the chapter 4.6.

### Fifth computational step

Part of the combustion chamber is loaded by the combustion pressure in the fifth step. Due to the lack of valves in the computational model, it is necessary to recalculate the pressure acting on the valve seats by means of the valve size and the seat contact surface. Engine load by combustion pressure is described in the chapter 4.7.

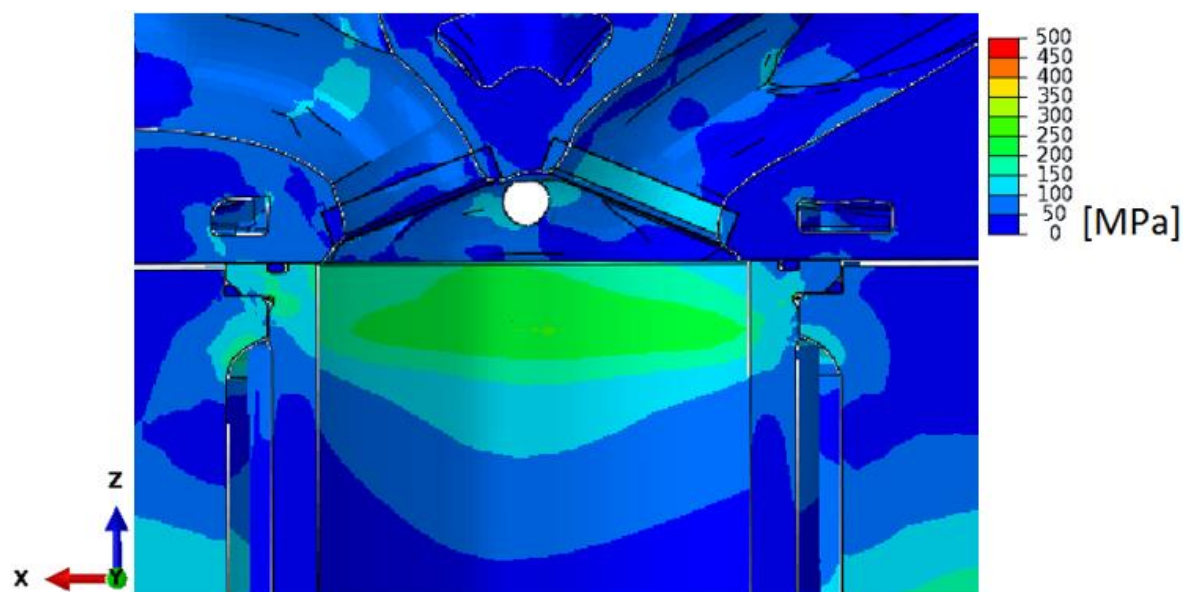


Figure 26: Stress during the Highest Combustion Pressure Variant A TSI Resistance 2

### Sixth computational step

The sixth step simulates engine after ignition. The combustion pressures cease to operate, but the engine is still heated to the operating temperature.

### Seventh computational step

In the last step, the engine is cooled to the initial laboratory temperature.

*Table 4: Boundary Conditions Summary*

Step 1	<ul style="list-style-type: none"> <li>• valve seats pressed into the cylinder head</li> <li>• valves guides pressed into the cylinder head</li> <li>• partial tightening of the screws</li> <li>• all parts are set to the initial laboratory temperature</li> </ul>
Step 2	<ul style="list-style-type: none"> <li>• tightening of the screws to the desired preload</li> </ul>
Step 3	<ul style="list-style-type: none"> <li>• screws are fixed</li> <li>• contacts between the cylinder liner and the engine block are turned on</li> </ul>
Step 4	<ul style="list-style-type: none"> <li>• operating temperatures are mapped to individual nodes</li> </ul>
Step 5	<ul style="list-style-type: none"> <li>• combustion chamber is loaded by the combustion pressure</li> </ul>
Step 6	<ul style="list-style-type: none"> <li>• combustion pressure cease to operate</li> </ul>
Step 7	<ul style="list-style-type: none"> <li>• engine is cooled to the initial laboratory temperature</li> </ul>

Table 4 shows the summary of the boundary conditions in the individual computational steps.

## 4.5 Contacts Between Parts

In a finite element analysis contact conditions are a special class of discontinuous constraint, allowing forces to be transmitted from one part of the model to another. The constraint is discontinuous because it is applied only when the two surfaces are in contact. When the two surfaces separate, no constraint is applied. The analysis has to be able to detect when two surfaces are in contact and apply the contact constraints accordingly. Similarly, the analysis must be able to detect when two surfaces separate and remove the contact constraints.

When surfaces are in contact, they usually transmit shear as well as normal forces across their interface. Thus, the analysis may need to take frictional forces, which resist the relative sliding of the surfaces into account. Coulomb friction is a common friction model used to describe the interaction of contacting surfaces. The model characterizes the frictional behavior between the surfaces using a coefficient of friction  $\mu$ .

[11]

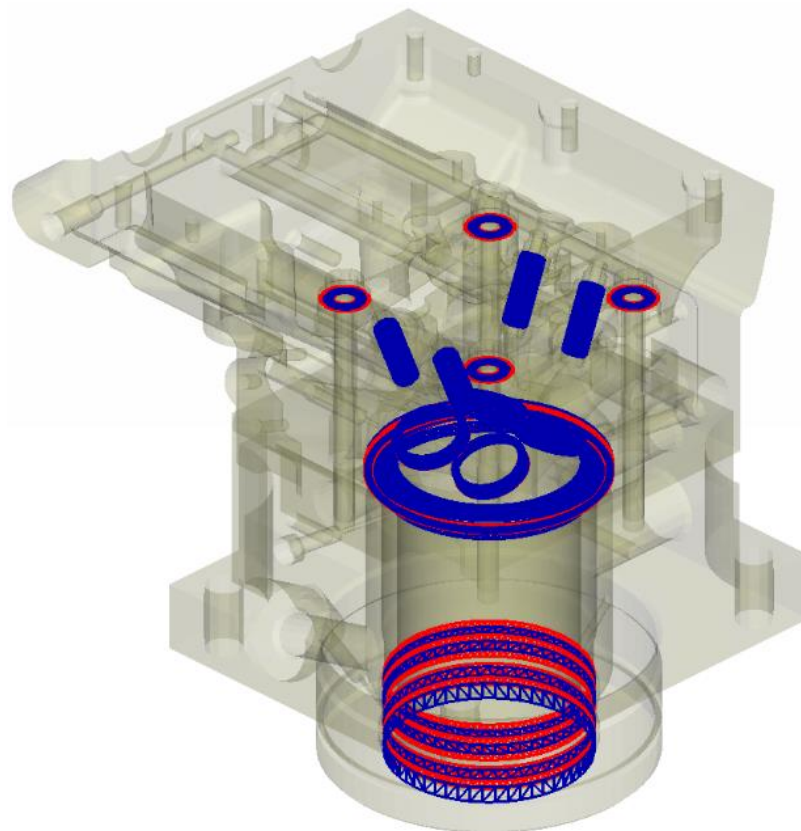


Figure 27: Contact Pairs in the Computational Model



There are 30 contact pairs in each variation of the computational model. In addition to four tie types of the contact pair, the coefficient of friction  $\mu$  between the parts is defined. The coefficient of friction  $\mu$  is set to 0.18 in contact between copper and steel, to 0.7 in contact between O-ring and steel and to 0.12 in all other contacts.

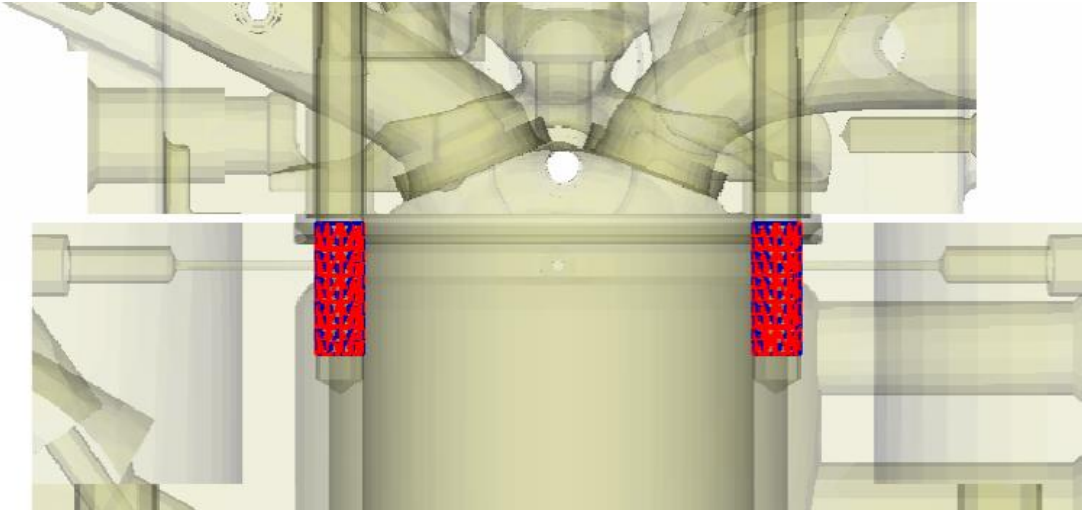


Figure 28: Tie Contact Pair

The tie constraint prevents surfaces initially in contact from penetrating, separating, or sliding relative to one another. This contact is used in our case after tightening the screws. The tie contact in the computational model simulates thread function.

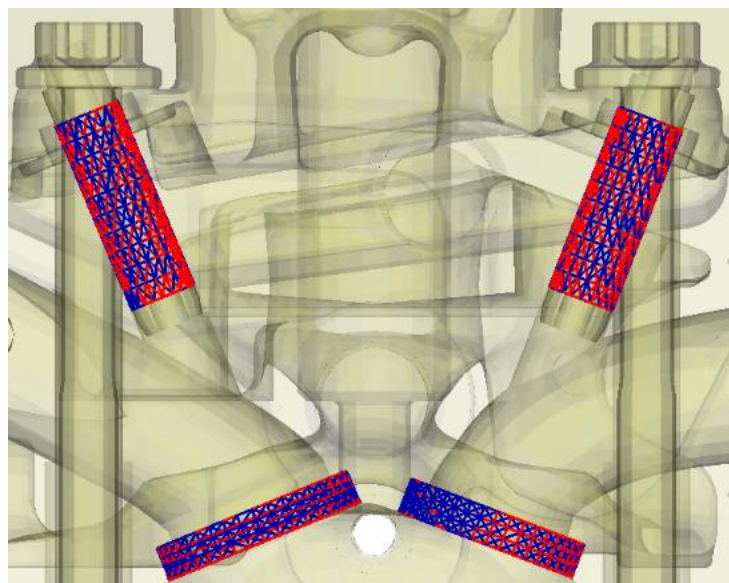
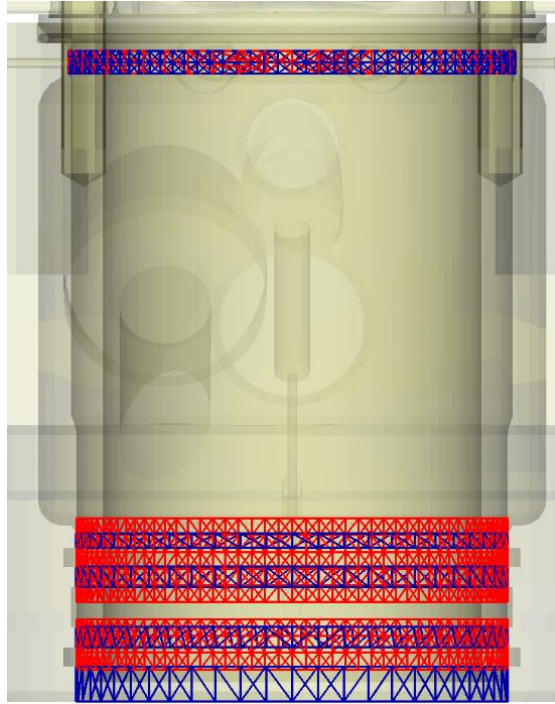


Figure 29: Contact Pair of the Valve Seats and the Valve Guides

The valve guides and valve seat are pressed with overlap. The overlap of the valve guides is 0.059 mm and the valve seat overlap is 0.105 mm.



*Figure 30: Contact Pair Cylinder Liner - Engine Block*

Figure 30 shows the contact pairs between the cylinder liner and the engine block, which are turned on in the third computational step at first. This is because the cylinder liner in the first two steps moves towards the engine block in the direction of the screws tightening. If these contact pairs were turned on from the start, the calculation would converge worse.

Table 5 shows an overview of the contacts used in the computational models for all variants. Marking of the contacts is described in the abbreviations list.

Table 5: Contacts Overview

Contact	Type of Contact	Friction [-]	Overlap [mm]	Available for Variants
ZK to ZKS_A1	standard	0.12	0	A/B1/B2
ZK to ZKS_A2	standard	0.12	0	A/B1/B2
ZK to ZKS_E1	standard	0.12	0	A/B1/B2
ZK to ZKS_E2	standard	0.12	0	A/B1/B2
ZK to VF_A1	standard	0.12	0.059	A/B1/B2
ZK to VF_A2	standard	0.12	0.059	A/B1/B2
ZK to VF_E1	standard	0.12	0.059	A/B1/B2
ZK to VF_E2	standard	0.12	0.059	A/B1/B2
ZK to SR_A1_A	standard	0.12	0.105	A/B1/B2
ZK to SR_A2_A	standard	0.12	0.105	A/B1/B2
ZK to SR_E1_A	standard	0.12	0.105	A/B1/B2
ZK to SR_E2_A	standard	0.12	0.105	A/B1/B2
ZK to SR_A1_R	standard	0.12	0	A/B1/B2
ZK to SR_A2_R	standard	0.12	0	A/B1/B2
ZK to SR_E1_R	standard	0.12	0	A/B1/B2
ZK to SR_E2_R	standard	0.12	0	A/B1/B2
BUCHSE to ZKG_01	standard	0.12	0	A/B1/B2
BUCHSE to ZKG_02	standard	0.12	0	A/B1/B2

BUCHSE to ZKG_03	standard	0.12	0	A/B1/B2
BUCHSE to ZKG_04	standard	0.12	0	A/B1/B2
BUCHSE to ZKG_05	standard	0.12	0	A/B1/B2
BUCHSE to ZKG_06	standard	0.12	0	A/B1/B2
BUCHSE to ZK_01	standard	0.12	0	A
BUCHSE to ZK_02	standard	0.12	0	A
O-RING GENERAL 01	general	0.7	0	A
O_RING GENERAL 02	general	0.7	0	A/B1/B2
ZKG to ZKS_A1	tie	0.12	0	A/B1/B2
ZKG to ZKS_A2	tie	0.12	0	A/B1/B2
ZKG to ZKS_E1	tie	0.12	0	A/B1/B2
ZKG to ZKS_E2	tie	0.12	0	A/B1/B2
BUCHSE to GA 01	standard	0.18	0	B1/B2
BUCHSE to GA 02	standard	0.18	0	B1
ZK to GA	standard	0.18	0	B1/B2

## 4.6 Thermal Field of the Engine

In order to verify functionality of the engine and the gaskets, it is necessary to know the thermal field of all parts in the engine. In our case we are interested in the thermal field of the engine block, cylinder liner, cylinder head, gaskets, screws, valve guides and valve seats.

For the calculation of the thermal field, the boundary conditions of the naturally aspirated engines are used first. In the other variants, the boundary conditions of the supercharged (TSI) version are used.

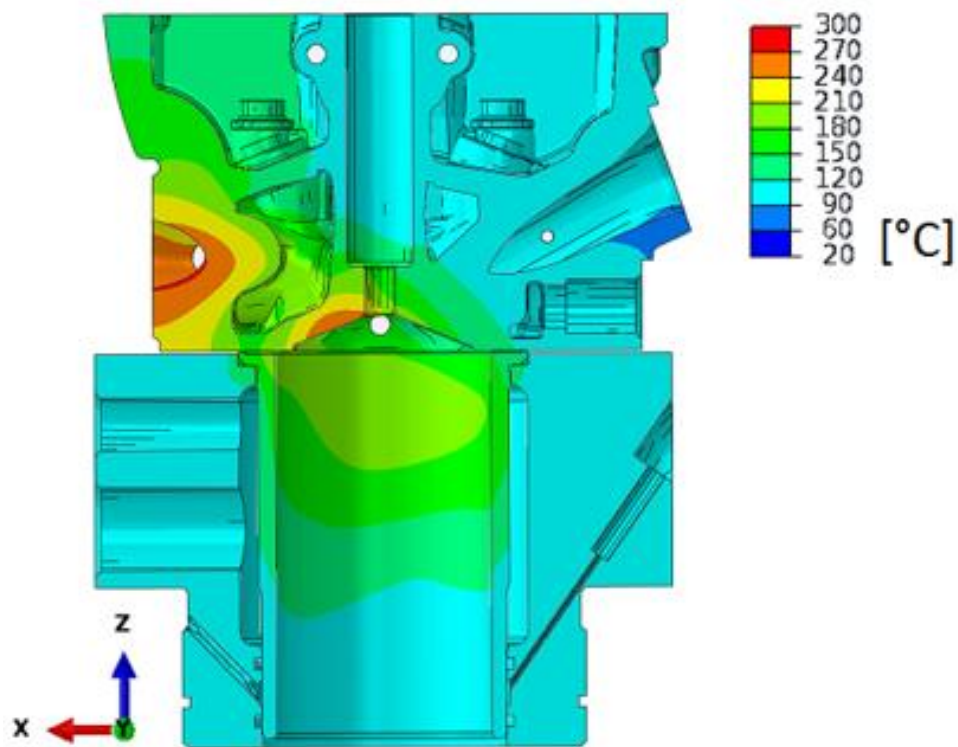


Figure 31: Temperature Field of the Engine Variant B1 TSI

It is possible to assign the temperature to the individual nodes of the model by using the STAR CCM+ program. These temperatures are exported to the input file for Abaqus. The temperature field is an important component for strength calculations.

The water input to the block and the cylinder head is defined by mass flow, density, dynamic viscosity, specific heat capacity, coefficient of the thermal conductivity and the Prandtl number.

The inlet flow rate in the engine block  $\dot{V}_{wb}$  is the same as the flow at the cylinder head inlet  $\dot{V}_{wh}$ .  $\dot{V}_{wb} = \dot{V}_{wh} = 20$  [l/min]. The density of water  $\rho_w$  is 1 [kg/l]. The inlet water temperature is 100 [°C]. The water outlet is defined by ambient pressure. Outlet pressure is 1 [bar].

$$\dot{m}_{wb} = \frac{\dot{V}_{wb} \cdot \rho_w}{60} = \frac{20 \cdot 1}{60} = 0,33 \text{ [kg/s]} \quad (4.1)$$

$$\dot{m}_{wh} = \dot{m}_{wb} = 0,33 \text{ [kg/s]} \quad (4.2)$$

$\dot{m}_{wb}$  – water mass flow in the engine block [kg/s]

$\dot{m}_{wh}$  – water mass flow in the cylinder head [kg/s]

Table 6: Coolant Parameters

Fluid	Density [kg/m <sup>3</sup> ]	Dynamic Viscosity [Pa·s]	Specific Heat Capacity [J/kg·K]	Coefficient of the Thermal Conductivity [W/m·K]	Prandtl Number	Mass Flow [kg/s]
water	1018	8.0422·10 <sup>-4</sup>	3650	0.443	0.9	0.33

On the outer side of the model, the ambient temperature and the heat transfer coefficient are set. It is assumed that the ambient engine temperature is 50 [°C]. The walls between the cylinder head and the engine block, which are separated by a narrow gap are set as adiabatic. The coolant temperature input is set to 100 [°C]. We considered the maximum engine load in the calculation of the temperature field.

Heat can be spread through conduction, convection and radiation. Thermal conduction is the transfer of heat (internal energy) by microscopic collisions of particles and movement of electrons within a body. Convection is the heat transfer due to bulk movement of molecules within fluids such as gases and liquids. Radiation is the transmission of energy in the form of waves or particles through space.

### 4.6.1 Thermal Resistances

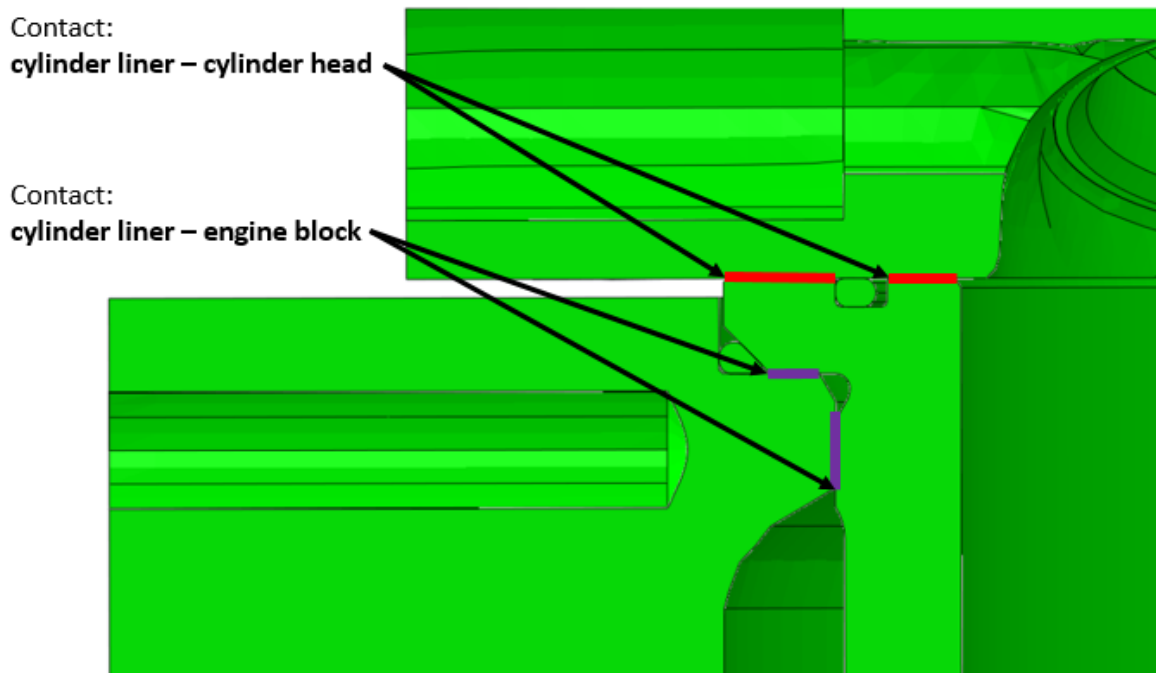


Figure 32: Contacts Containing Thermal Resistances

For variant A, which uses 2 O-rings, three subvariants are considered. In the first subvariant, the ideal contact between the cylinder liner, the cylinder head and the engine block is envisaged. In the second subvariant, which is referred to as Resistance 1, the thermal resistance between the cylinder liner and the cylinder head is considered. In the third subvariant, which is referred to as Resistance 2, a thermal resistance between the cylinder liner and the cylinder head and also between the cylinder liner and the engine block is considered.

$$R = \frac{d}{\lambda} [m^2K/W] \quad (4.3)$$

The thermal resistance  $R$  is set to  $4 \cdot 10^{-4} m^2K/W$ . This value corresponds to the thermal resistance produced by a  $1.04 \times 10^{-5} m$  wide air layer. The thermal conductivity of the air is  $\lambda = 0.026 W \cdot m^{-1} \cdot K^{-1}$ . The width of the air layer is indicated by  $d$ .

Table 7 shows the summary of the computational variants. The cylinder liner is marked as a BUCHSE, the engine block as ZKG and the cylinder head as ZK in the table.

Table 7: Summary of the Computational Variants

Variant	Type of Engine	Combustion Pressure [bar]	Thermal Resistances
MPI_IDEAL_CONTACT	naturally aspirated	70	-
MPI_RESISTANCE_1	naturally aspirated	70	BUCHSE – ZK
MPI_RESISTANCE_2	naturally aspirated	70	BUCHSE – ZK BUCHSE – ZKG
TSI_IDEAL_CONTACT	supercharged	130	-
TSI_RESISTANCE_1	supercharged	130	BUCHSE – ZK
TSI_RESISTANCE_2	supercharged	130	BUCHSE – ZK BUCHSE – ZKG

#### 4.6.2 O-ring Temperatures

The Viton O-ring that seals water is the same for all variants. It is an O-ring with an internal diameter of 96 mm and a thickness of 2 mm. Maximum temperatures for individual variants range from 148 °C to 186 °C. The Viton O-ring that seals the combustion chamber is used only in variant A. It is an O-ring with an internal diameter of 84 mm and a thickness of 2 mm. Maximum temperatures for individual subvariants range from 160 °C to 208 °C.

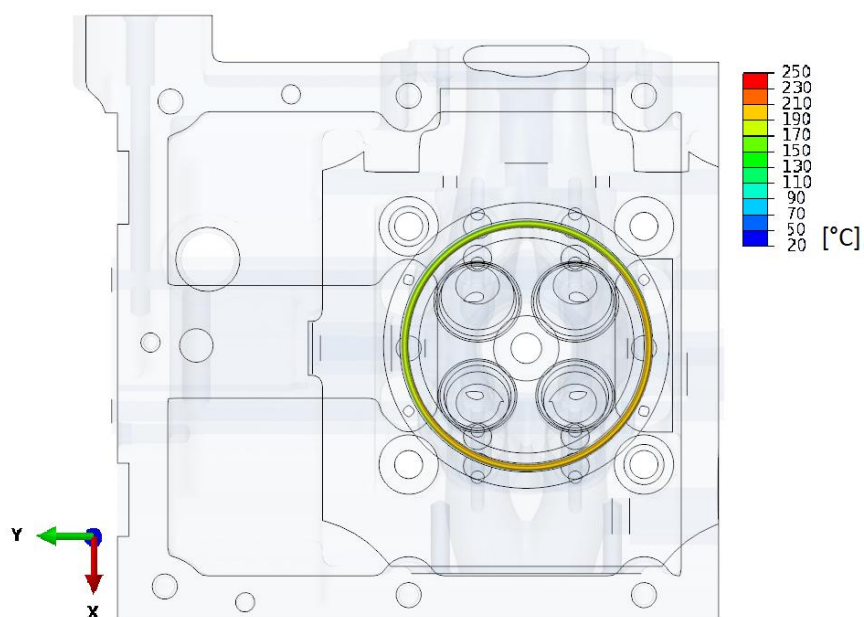


Figure 33: O-ring Combustion A TSI Resistance 2



Table 8 shows the maximum and minimum O-ring temperatures for variant A.

The O-ring reaches the highest temperatures on the side where the exhaust valves are. The cylinder head is heated to a higher temperature on the side of the exhaust valves. The heat from the cylinder liner is better transferred to the cooler part of the cylinder head.

Table 8: O-ring Temperatures Variant A

	O-ring Water		O-ring Combustion	
	min. temperature	max. temperature	min. temperature	max. temperature
A_MPI_IDEAL_CONTACT	109 °C	148 °C	114 °C	160 °C
A_MPI_RESISTANCE_1	114 °C	148 °C	114 °C	166 °C
A_MPI_RESISTANCE_2	106 °C	164 °C	116 °C	182 °C
A_TSI_IDEAL_CONTACT	113 °C	168 °C	118 °C	185 °C
A_TSI_RESISTANCE_1	120 °C	165 °C	119 °C	188 °C
A_TSI_RESISTANCE_2	108 °C	186 °C	121 °C	208 °C

An ideal contact between the cylinder head and the cylinder liner is considered for variants B1 and B2, which seals the combustion chamber with a copper gasket. Copper is a metal with high heat conductivity. Copper is also a malleable metal, so that the surface imperfection of the cylinder head and cylinder liners will have no effect.

Tables 9 and 10 shows the maximum and minimum O-ring temperatures for variants B1 and B2.

Table 9: O-ring Temperatures Variant B1

	O-ring Water	
	min. temperature	max. temperature
B1_MPI	110 °C	148 °C
B1_TSI	114 °C	168 °C

Table 10: O-ring Temperatures Variant B2

	O-ring Water	
	min. temperature	max. temperature
B2_MPI	109 °C	148 °C
B2_TSI	113 °C	168 °C

All O-ring temperatures are within the allowed limits. The maximum allowed O-ring temperature is 250 °C. This ensures that no O-ring exposed to increased wear in all possible working conditions.

### 4.6.3 Cylinder Liner Temperatures

The peak temperature of the cylinder liner is achieved at the top of the liner on the side of the exhaust valves. The highest temperature of the fuel mixture is reached due to the highest pressure. The highest pressure in the cylinder is at the moment the piston is 11 ° behind the upper dead center in the upper part of the cylinder liner. Another reason for the higher temperature in the top of the cylinder is that it is most distant from the water that cools the engine.

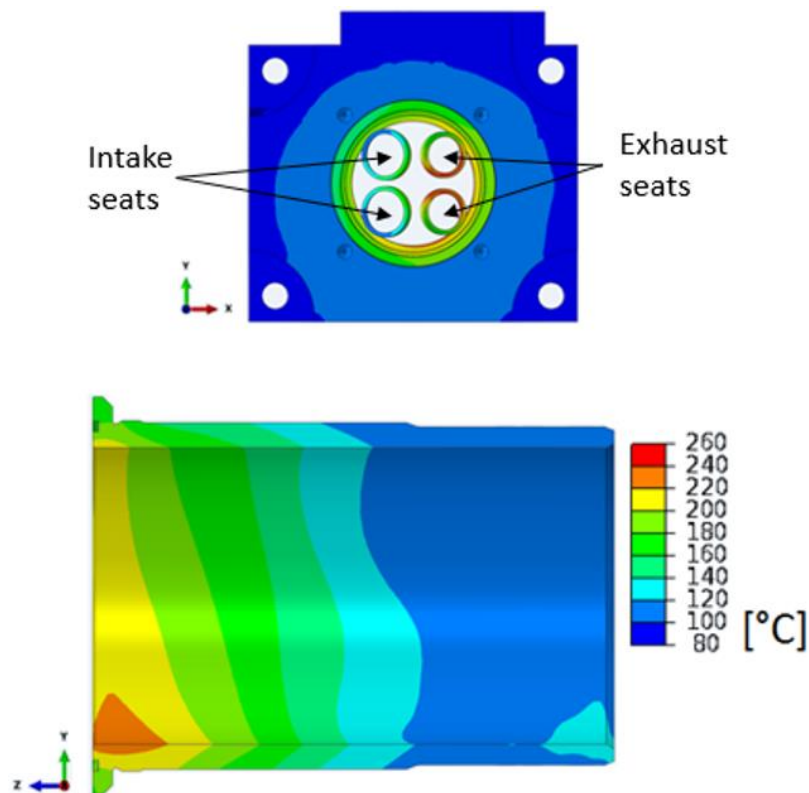


Figure 34: Cylinder Liner A TSI Resistance 2 Temperature

The heating of the cylinder liner is not symmetrical because the water that cools the cylinder liner also does not flow symmetrically. This is due to the geometry of the engine block.

The increased thermal resistance of contact between the cylinder liner, the cylinder head and the engine block has a large effect on the maximum temperature of the cylinder liner variant A. Increased thermal resistance will make it more difficult for heat to drain away from the top of the cylinder liner, which is most heat-stressed. The cylinder liner variant A has approximately 20 degrees higher maximum temperature than the B1 and B2 variants that transfer heat through the copper gasket.

Table 11 shows the maximum and minimum cylinder liner temperatures for variant A.

Table 11: Cylinder Liner A Temperature

	<b>Cylinder Liner A</b>	
	min. temperature	max. temperature
A_MPI_IDEAL_CONTACT	104 °C	177 °C
A_MPI_RESISTANCE_1	104 °C	187 °C
A_MPI_RESISTANCE_2	104 °C	202 °C
A_TSI_IDEAL_CONTACT	104 °C	207 °C
A_TSI_RESISTANCE_1	104 °C	215 °C
A_TSI_RESISTANCE_2	105 °C	235 °C

Both variants B1 and B2 have nearly identical temperatures of the cylinder liner. The highest achievable temperature of these cylinder liners is 207 °C.

Table 12: Cylinder Liner B1 Temperature

	<b>Cylinder Liner B1</b>	
	min. temperature	max. temperature
B1_MPI	104 °C	177 °C
B1_TSI	104 °C	207 °C

Table 13: Cylinder Liner B2 Temperature

	<b>Cylinder Liner B2</b>	
	min. temperature	max. temperature
B2_MPI	104 °C	177 °C
B2_TSI	104 °C	207 °C

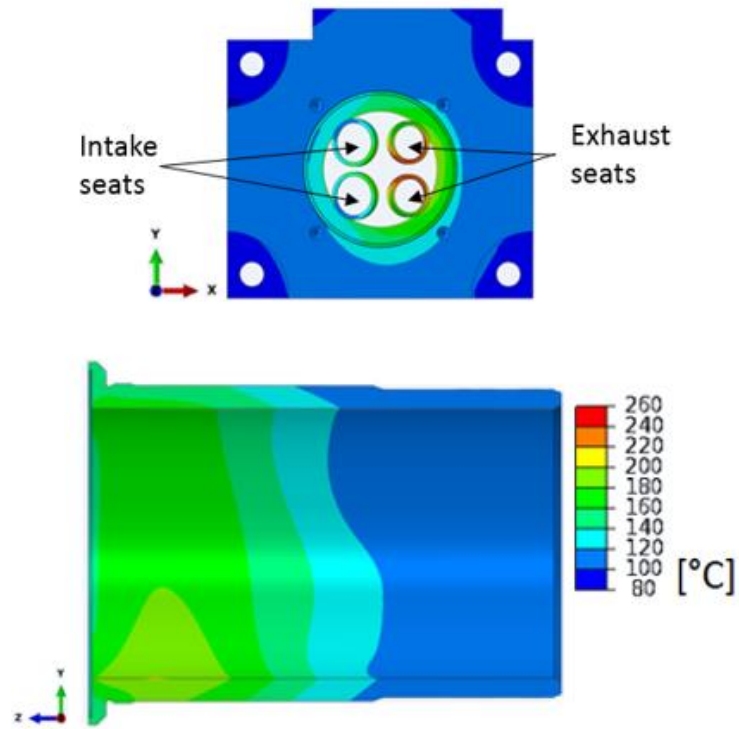


Figure 35: Cylinder Liner B1 TSI Temperature

Tables 12 and 13 shows the maximum and minimum cylinder liner temperatures for variants B1 and B2.

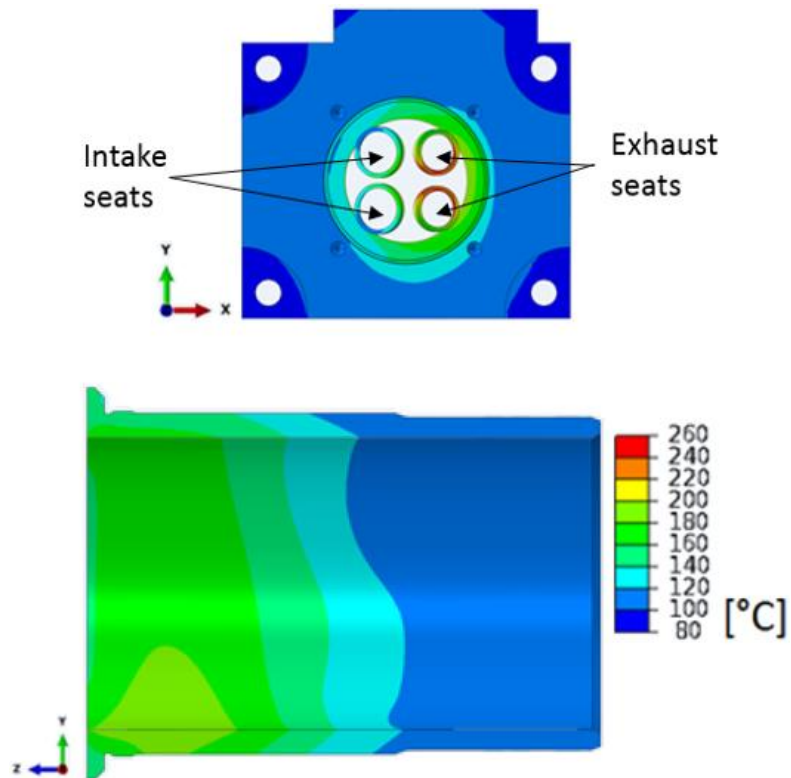


Figure 36: Cylinder Liner B2 TSI Temperature

## 4.7 Effect of Combustion Pressure

The model of a single-cylinder experimental engine is loaded by the combustion pressure in the fifth computational step. Two values of the maximum combustion pressure are counted. In the first case, it is a naturally aspirated variant that achieves a maximum combustion pressure of 70 MPa. In the second case, it is a supercharging variant that achieves a maximum combustion pressure of 130 MPa. The pressure is applied to the cylinder wall at the top, where the piston is 11 degrees behind the top dead center. Pressure further affects the part of the cylinder head that is part of the combustion chamber. It was necessary to calculate the pressure on the seats of the valve seats because the intake and exhaust valves are not part of the model.

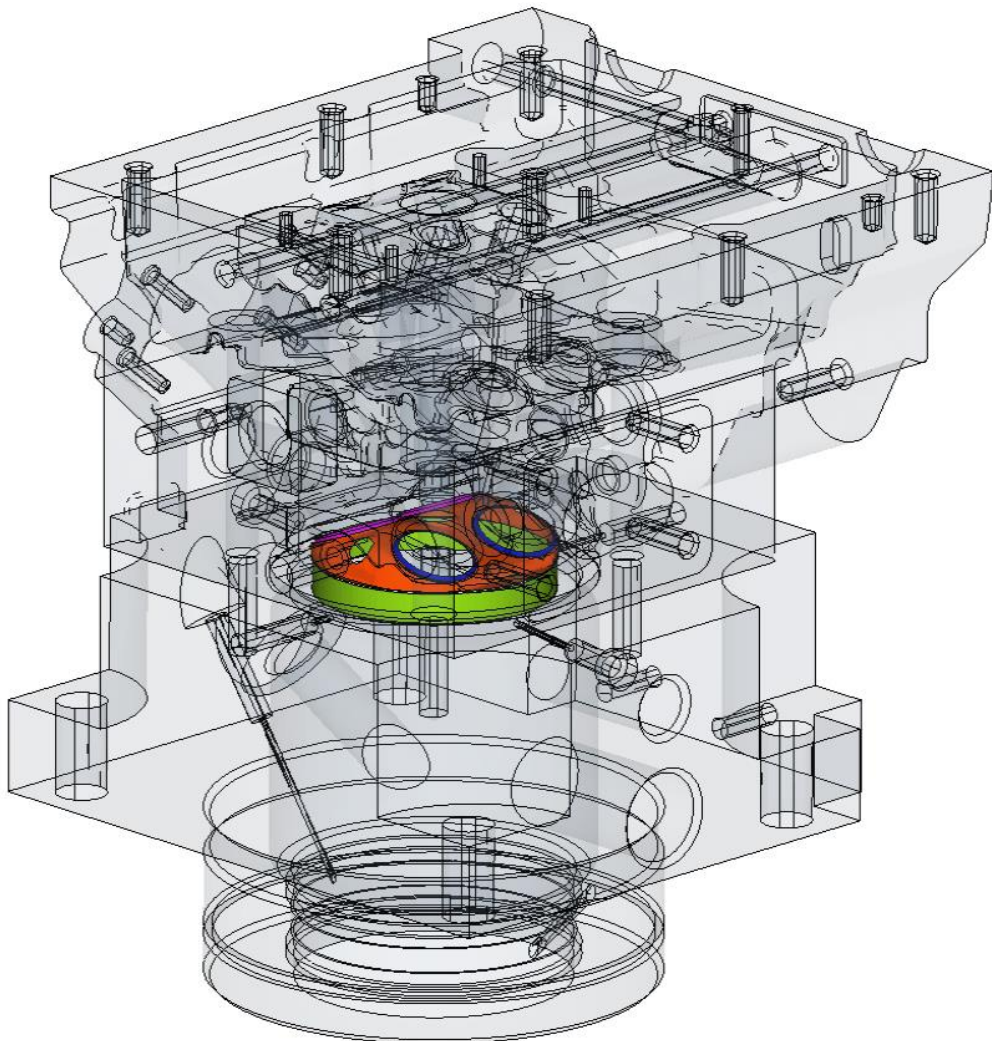


Figure 37: Set of Elements Loaded by the Combustion Pressure

The Figure 37 shows which sets of elements are loaded by the combustion pressure. Table 14 shows the values of pressures acting on the individual locations in the cylinder.

Table 14: Combustion Chamber Pressures

	Cylinder Wall	Cylinder Head	Intake Seat	Exhaust Seat
MPI	7 [MPa]	7 [MPa]	36 [MPa]	30.5 [MPa]
TSI	13 [MPa]	13 [MPa]	67 [MPa]	56.7 [MPa]

#### 4.7.1 Leakage Check of the O-ring for the Combustion Chamber

The Viton O-ring of hardness of 80 ShA can seal the pressure up to 200 bar. The maximum clearance of the sealing surfaces cannot be greater than 0.1mm. This means the distance between the cylinder liner and the cylinder head, which sticks to each other after assembly. The combustion pressure in the cylinder lifts the cylinder head when the mixture is ignited. The Figure 38 shows the groove for the O-ring and the face of the cylinder head that pushes the O-ring. The lifting of the cylinder head is reflected in the direction Z.

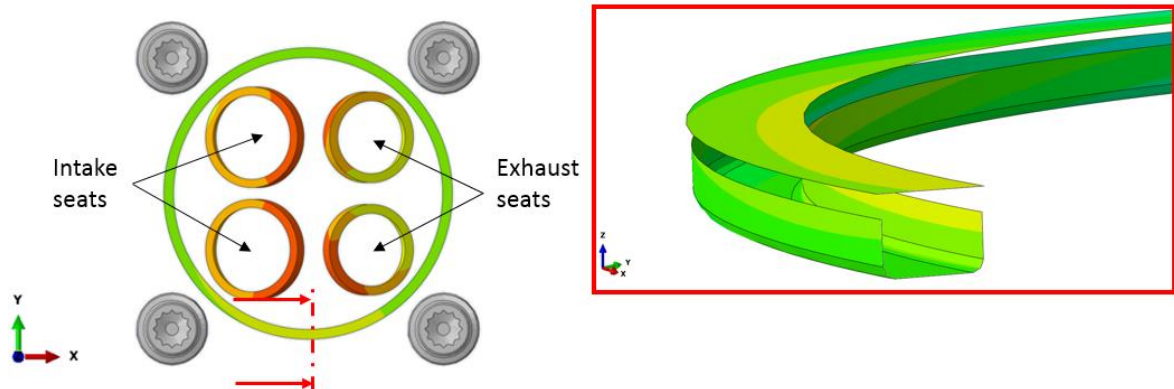


Figure 38: Groove for the O-ring of the Sealing Combustion Chamber

Table 15 shows the lift of the cylinder head as soon as the combustion pressure starts to occur in the cylinder. The highest cylinder head lift of 0.004 mm ensures that the O-ring seals the combustion chamber without any problems. The highest lift of the cylinder head is at the place farthest from the screw.

Table 15: Lift the Cylinder Head Relative to the Cylinder Liner

Variant A	Displacement [mm]	Limit [mm]
A_MPI_IDEAL_CONTACT	0.002	0.1
A_MPI_RESISTANCE_1	0.003	
A_MPI_RESISTANCE_2	0.003	
A_TSI_IDEAL_CONTACT	0.003	
A_TSI_RESISTANCE_1	0.003	
A_TSI_RESISTANCE_2	0.004	

## 4.8 Stress of the Upper Mounting of the Cylinder

The temperature of the components, which is included in the calculations much affects the stress. Some components are most loaded with burned mixture in the cylinder in the computational step five. Some components are loaded the most after the mixture is ignited, when the engine is warmed to the operating temperature but the pressure does not act in the cylinder in the computational step six.

### 4.8.1 Stress of the Cylinder Head

The cylinder head screws act on the cylinder head by tightening to the required tightening torque. The combustion pressure in the cylinder also affects the stress on the cylinder head. The most stressed place is under the screw head. The greatest stress is when the maximum combustion pressure is applied. The maximum pressure is in the computational step five. The maximum stress is in the variant A TSI Resistance 2. The maximum stress exceeds the yield strength, so it is necessary to check how large the cumulative plastic deformations of the cylinder head are. Since the compressive yield strength values are not available, the tensile yield strength is calculated. Tensile yield strength is always lower than compressive yield strength. The maximum stress values for each variant are described in the table 16. The gray sections in the Figure 39 show where the yield strength is exceeded.

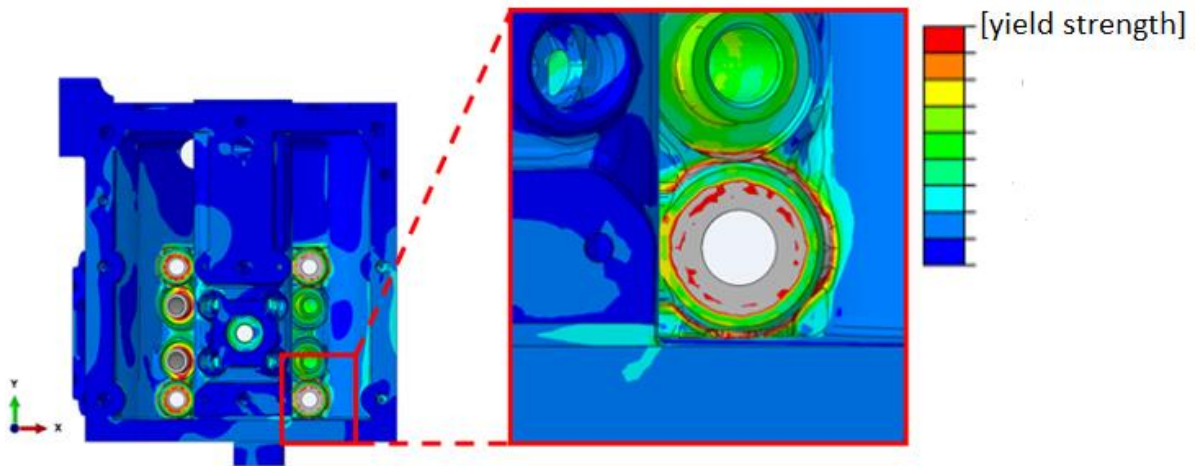


Figure 39: Stress of the Cylinder Head A TSI Resistance 2

Table 16: Maximum Stress of the Cylinder Head from the Screw

Cylinder Head	Maximum Stress [MPa]
A_MPI_IDEAL_CONTACT	230
A_MPI_RESISTANCE_1	230
A_MPI_RESISTANCE_2	230
B1_MPI	230
B2_MPI	230
A_TSI_IDEAL_CONTACT	232
A_TSI_RESISTANCE_1	232
A_TSI_RESISTANCE_2	237
B1_TSI	232
B2_TSI	233

Figure 40 shows the contact pressure between the copper gasket and the cylinder head. The contact pressure is the same for the variant B1 and for the variant B2. The highest contact pressure is in the sixth computational step. On the other hand the lowest contact pressure is in the fifth computation step as the pressure lifts the cylinder head and relieves the copper gasket. The cylinder head is the most loaded in places closest to the screws and on the edge of the copper gasket. The yield strength exceeds contact pressure only at the edge of the copper gasket. In other places the contact pressure is well below the yield strength. Since the compressive yield strength values are not available, the tensile yield strength is calculated. There is no permanent deformation of the cylinder head from the copper gasket in this case.



Analytical calculation of the contact pressure between the copper gasket and the cylinder head:

$$F = 4 \cdot 31\,000 \text{ N} = 124\,000 \text{ [N]} \quad (4.4)$$

$$S_{Cu} = \frac{\pi \cdot (95.5^2 - 76^2)}{4} = 2627 \text{ [mm}^2\text{]} \quad (4.5)$$

$$\sigma_{Cu} = \frac{F}{S_{Cu}} = 47.2 \text{ [MPa]} \quad (4.6)$$

F is the force of the four preload cylinder head screws,  $S_{Cu}$  is the copper gasket cross-section and the  $\sigma_{Cu}$  is the contact pressure between the copper gasket and the cylinder head.

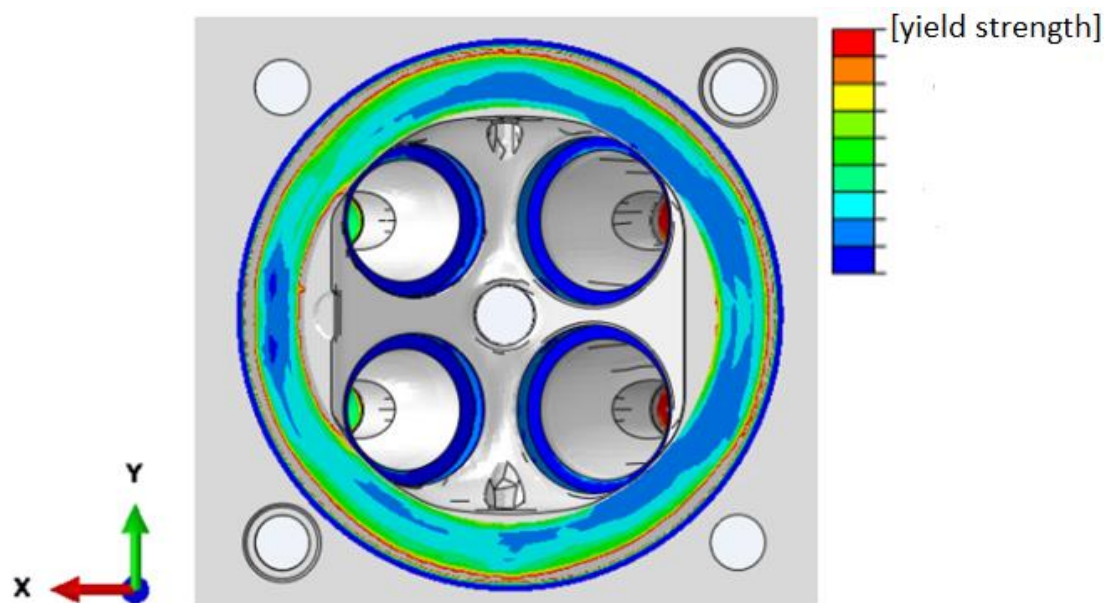


Figure 40: Contact Pressure between the Cylinder Head and the Copper Gasket

## 4.8.2 Stress of the Cylinder Liner

The cylinder liner is most stressed when the engine is warmed to operating temperature and does not cause combustion pressure inside the cylinder. This state describes the sixth computational step. This is due to the combustion pressure not lifting the cylinder head and therefore the load on the cylinder liner has the greatest value.

The yield strength of the material EN-GJL-350 is 228-285 MPa. The lowest value of 228 MPa is considered in the calculation.

Figure 41 shows the cross-section view of the place with the highest stress of the cylinder liner variant A. Critical places that exceed the yield strength are in the groove for the O-ring and on the outside notch. The highest stress in the material is generated on the side where the exhaust valves are located because the highest temperature is at these locations. The place the highest stress occurs is located close to the cylinder head screw. The cylinder liner variant A must be checked for safety and fatigue and the magnitude of the cumulative plastic deformation.

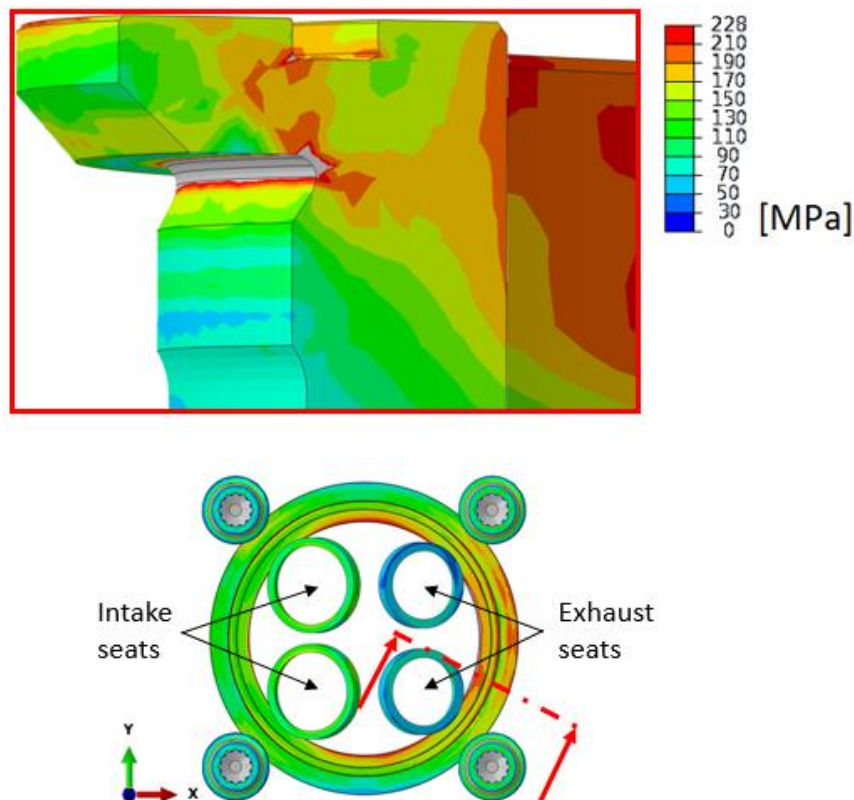


Figure 41: Stress of the Cylinder Liner A TSI Resistance 2

Table 17 shows the highest stresses for variant A.

Table 17: Maximum Stress of the Cylinder Liner A

Cylinder Liner Variant A	Maximum Stress [MPa]
A_MPI_IDEAL_CONTACT	290
A_MPI_RESISTANCE_1	294
A_MPI_RESISTANCE_2	300
A_TSI_IDEAL_CONTACT	311
A_TSI_RESISTANCE_1	313
A_TSI_RESISTANCE_2	313

Figure 42 shows the cross-section view of the place with the highest stress of the cylinder liner variant B1. Critical places that exceed the yield strength are on the outside notch. The highest stress in the material is generated on the side where the exhaust valves are located because the highest temperature is at these locations as in the variant A. The place the highest stress occurs is located close to the cylinder head screw. The cylinder liner variant B1 must be checked for safety and fatigue and the magnitude of the cumulative plastic deformation.

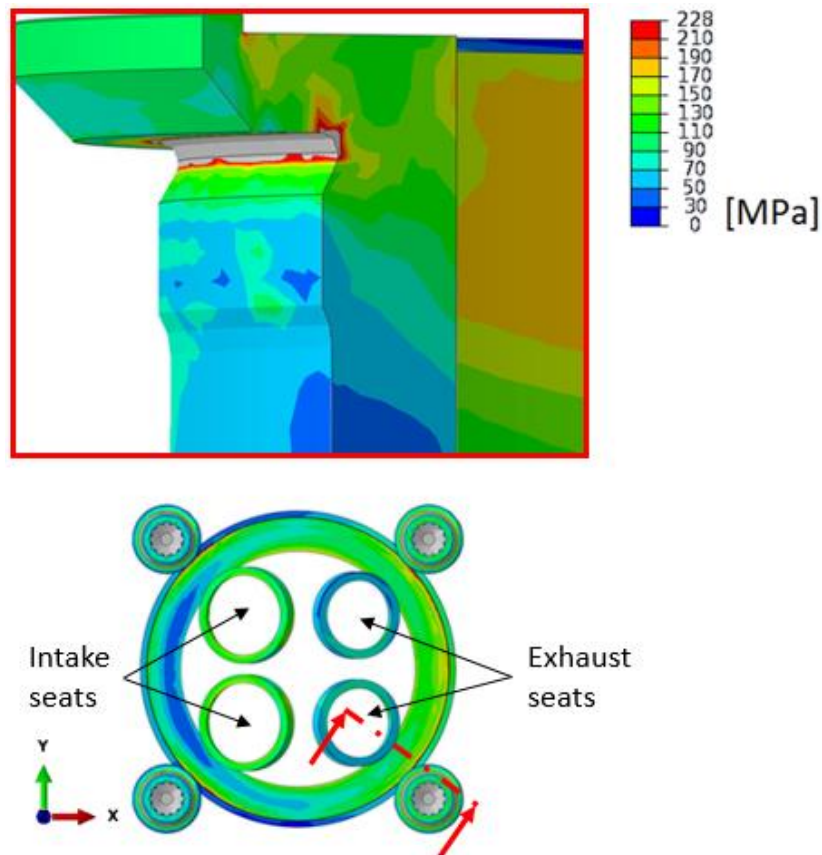


Figure 42: Stress of the Cylinder Liner B1 TSI

Table 18 shows the highest stresses for variant B1.

Table 18: Maximum Stress of the Cylinder Liner B1

Cylinder Liner Variant B1	Maximum Stress [MPa]
B1_MPI	267
B1_TSI	305

Figure 43 shows the contact pressure between the copper gasket and the cylinder liner variant B1. The highest contact pressure is in the sixth computational step. The cylinder liner is the most loaded in places closest to the screws and on the edge of the copper gasket. The yield strength 228 MPa exceeds contact pressure only at the edge of the copper gasket. In other places the contact pressure is well below the yield strength. Since the compressive yield strength values are not available, the tensile yield strength is calculated. There is no permanent deformation of the cylinder liner from the copper gasket in this case. Analytical contact pressure calculation is the same as in the chapter 4.8.1.  $\sigma_{Cu} = 48.2$  MPa.

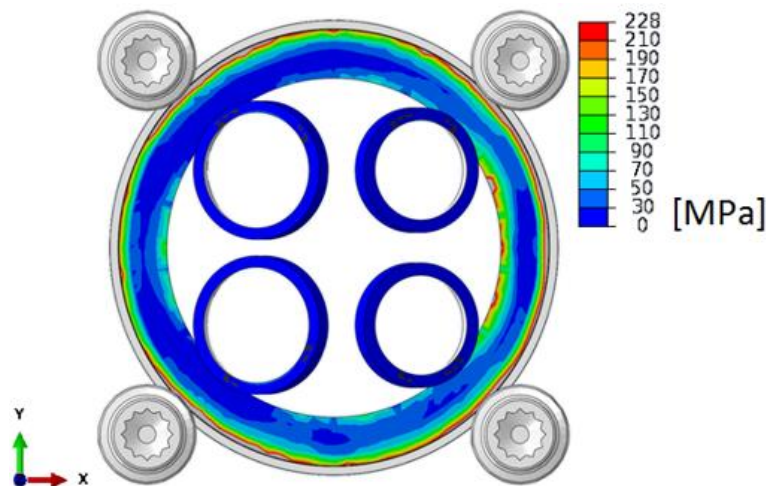


Figure 43: Cylinder Liner B1 TSI Contact Pressure

Figure 44 shows the cross-section view of the place with the highest stress of the cylinder liner variant B2. Critical places that exceed the yield strength are on the outside notch. The highest stress in the material is generated on the side where the exhaust valves are located because the highest temperature is at these locations as in the variants A and B1. The place the highest stress occurs is located close to the cylinder head screw. The cylinder liner variant B2 must be checked for safety and fatigue and the magnitude of the cumulative plastic deformation.

Table 19 shows the highest stresses for variant B2.

Table 19: Maximum Stress of the Cylinder Liner B2

Cylinder Liner Variant B2	Maximum Stress [MPa]
B2_MPI	284
B2_TSI	305

Figure 45 shows the contact pressure between the copper gasket and the cylinder liner variant B2. This variant B2 is loaded in the same way as B1. Both variants have the same critical points for the same reasons.

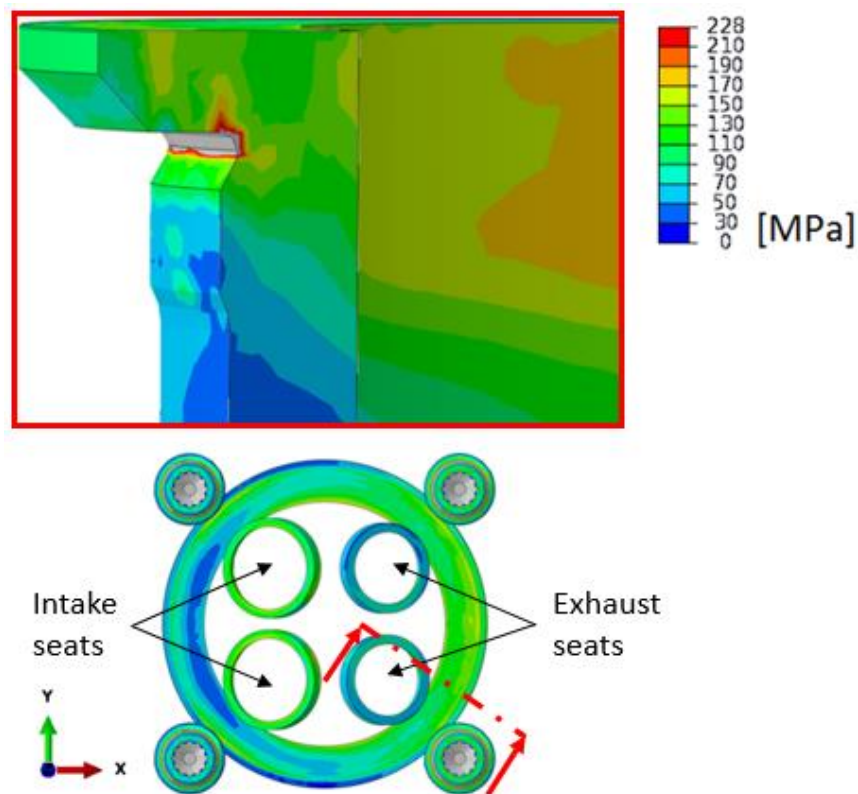


Figure 44: Stress of the Cylinder Liner B2 TSI

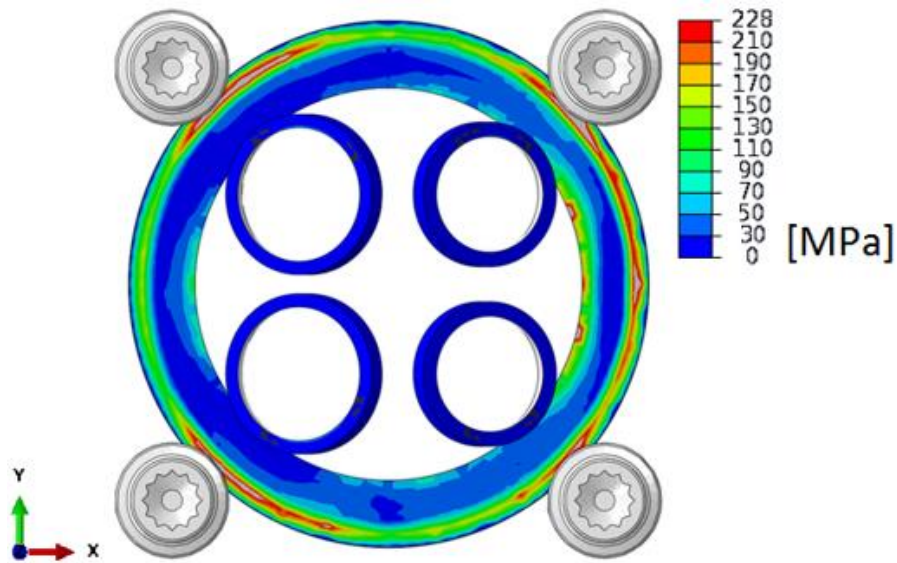


Figure 45: Cylinder Liner B2 TSI Contact Pressure

All cylinder liner variants have approximately the same peak of stress on the outside notch. For the cylinder liner in variant A, it is apparent that the stress between the groove for the O-ring and the outer notch is higher than for the remaining variants.

#### 4.8.3 Stress of the Copper Gasket

Figure 46 shows the locations of the highest stress of the copper gasket. The copper gasket is the most loaded in the sixth computational step because the engine is warmed to the operating temperature and the cylinder head is not lifted by the combustion pressure. The place the highest stress occurs is located close to the cylinder head screw. Another influence on the high stress of the copper gasket is that it has a high temperature which is higher on the side of the exhaust valves.

Compressive yield strength of the copper is 217 MPa.

[14]

The yield strength is exceeded only at the edge. This prevents the screws being released, which would be caused by large plastic deformations. Stresses in the copper gasket are the same for both variants B1 and B2.

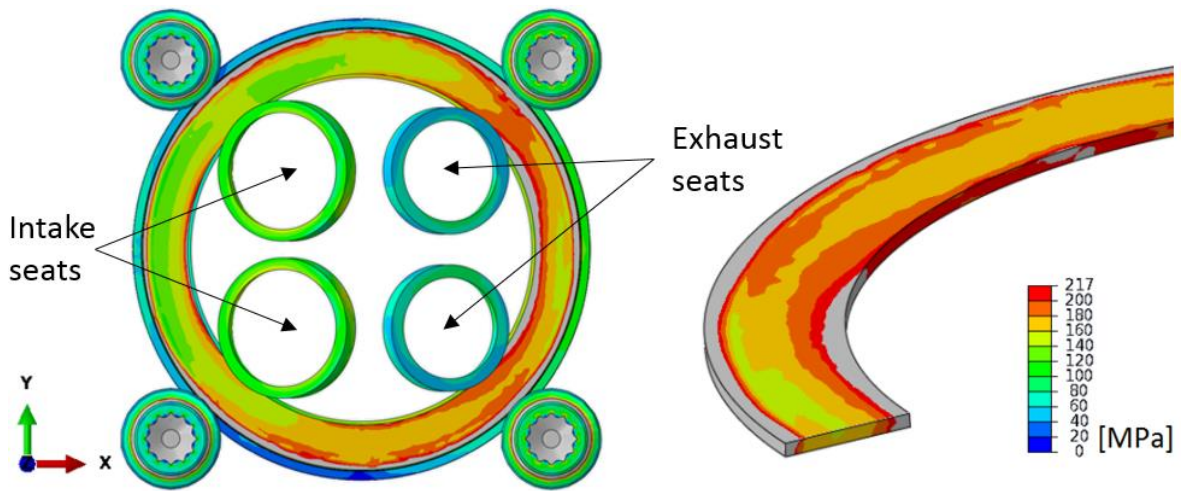


Figure 46: Stress of the Copper Gasket

#### 4.8.4 Stress of the Engine Block

The most stressed part of the engine block is in places where the engine block is in contact with the cylinder liner. The cylinder liner pushes the engine block in the axial direction Z. This is caused by the pretension of the screws. The engine block is most loaded in the sixth computational step because the engine is warmed to the operating temperature and the cylinder head is not lifting by the combustion pressure.

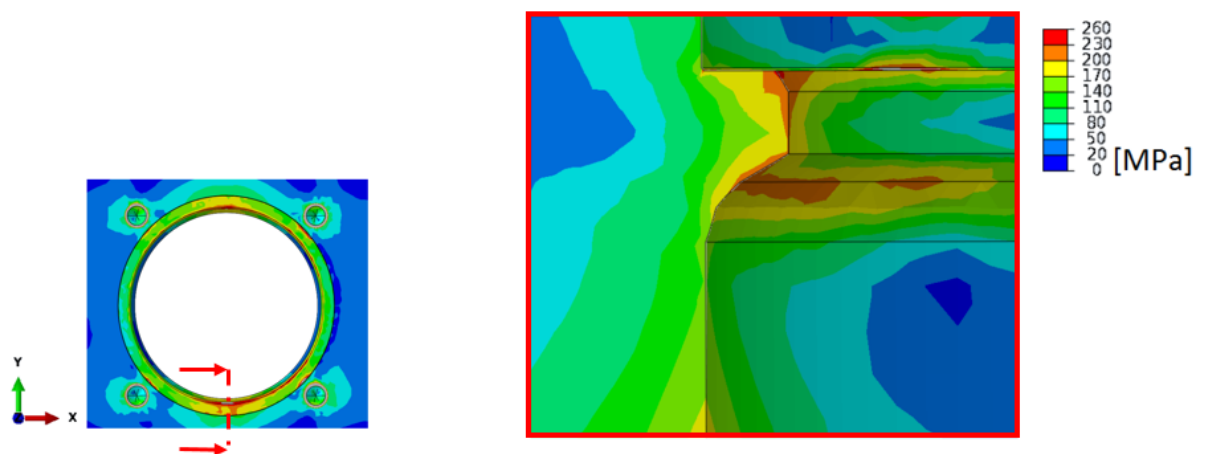


Figure 47: Stress of the Engine Block

Yield strength of the engine block material is 260 MPa. The yield strength is not exceeded.

[15]

**Analytical calculation of the contact pressure between the engine block and the cylinder liner:**

$$F = 4 \cdot 31\,000 \text{ N} = 124\,000 \text{ [N]} \quad (4.7)$$

$$S_{EB-CL} = \frac{\pi \cdot (95^2 - 89,7^2)}{4} = 769 \text{ [mm}^2\text{]} \quad (4.8)$$

$$\sigma_{EB-CL} = \frac{F}{S_{EB-CL}} = 161 \text{ [MPa]} \quad (4.9)$$

F is the force of the four preloaded cylinder head screws,  $S_{EB-CL}$  is the surface of the contact engine block and cylinder liner and the  $\sigma_{EB-CL}$  is the contact pressure between the engine block and the cylinder liner.

## 4.9 FEMFAT Safety Calculations

Fatigue safety calculations were performed in the FEMFAT program. This program simulates cyclic loading of the components. The components load simulation consisted in repeating computational steps five (ignition of the mixture) and six (after ignition of the mixture). This simulation describes the largest engine load for the all variants. The calculation settings in the program were set identically as for fatigue calculations for the engine components in ŠKODA-AUTO.



#### 4.9.1 Safety Factor of the Screw

Figure 48 shows where the lowest safety factor is on the screw. The critical point is under the screw head. The lowest possible safety factor of the screw which can be considered as permissible is 1.3. The worst is the minimum safety factor of the variant B2 TSI. Minimum safety factor of the variant B2 TSI is 2.35. This calculation proved that the proposed M9 screws with strength class 12.9 can be used for all variants.

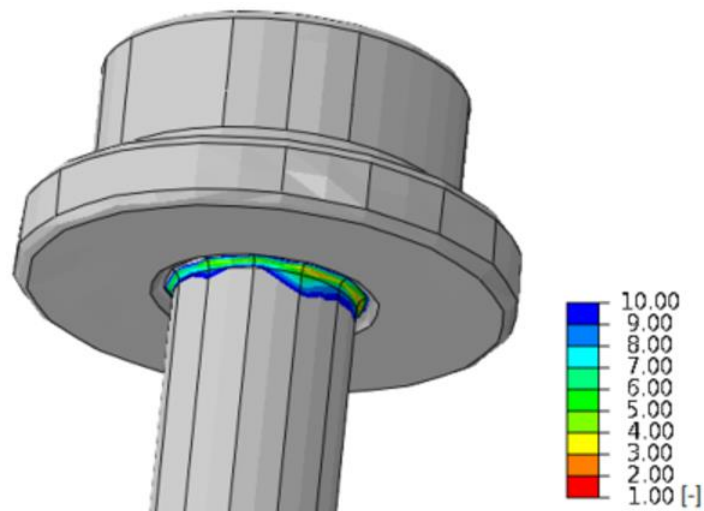


Figure 48: Cylinder Head Screw Minimum Safety Factor

Table 20 shows the minimum screw safety factor for each variant. Differences in minimum safety factors for each variant are due to different values of maximum combustion pressure and also to different temperatures in the engine.

Table 20: Cylinder Head Screw Minimum Safety Factor

Cylinder Head Screw	Minimum Safety Factor [-]
A_MPI_IDEAL_CONTACT	5.01
A_MPI_RESISTANCE_1	5.04
A_MPI_RESISTANCE_2	4.96
B1_MPI	4.53
B2_MPI	4.51
A_TSI_IDEAL_CONTACT	2.59
A_TSI_RESISTANCE_1	2.61
A_TSI_RESISTANCE_2	2.57
B1_TSI	2.36
B2_TSI	2.35

### 4.9.2 Safety Factor of the Cylinder Liner

The lowest possible safety factor of all the cylinder liners made from material EN-GJL-350 which can be considered as permissible is 1.3.

Figure 49 shows where the lowest safety factor is on the cylinder liner variant A. The critical point is in the groove for the O-ring. The lowest safety factor is on the side of the exhaust valves because of the higher temperatures. The worst is the minimum safety factor of the variant A TSI Resistance 2. The minimum safety factor of the variant A TSI Resistance 2 is 2.78. This calculation proved that the proposed cylinder liner variant A made from EN-GJL-350 can be used.

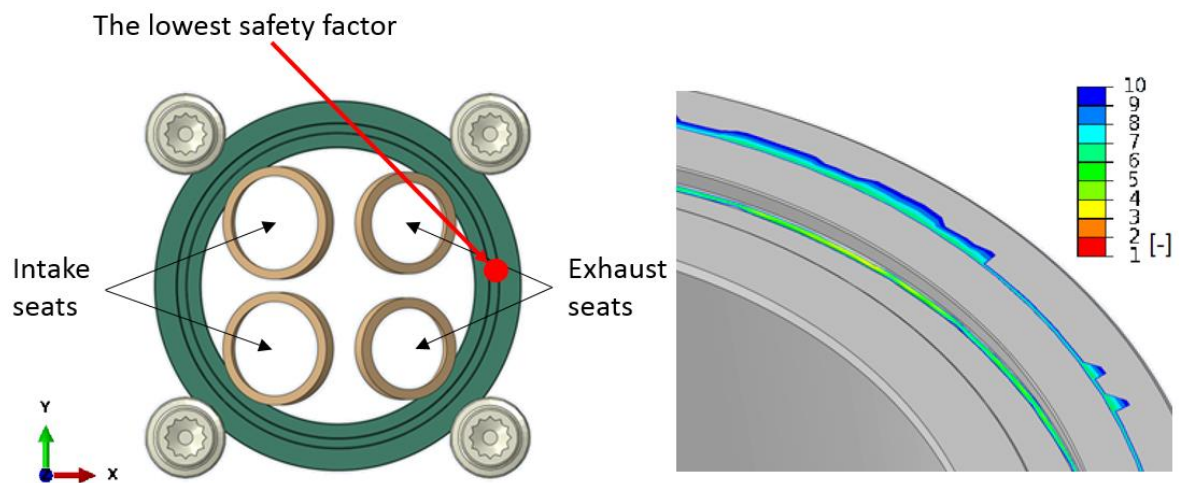


Figure 49: Cylinder Liner A Minimum Safety Factor

Table 21 shows the minimum cylinder liner variant A safety factor for each variant.

Table 21: Cylinder Liner A Minimum Safety Factor

Cylinder Liner Variant A	Minimum Safety Factor [-]
A_MPI_IDEAL_CONTACT	5.25
A_MPI_RESISTANCE_1	5.25
A_MPI_RESISTANCE_2	5.08
A_TSI_IDEAL_CONTACT	2.87
A_TSI_RESISTANCE_1	2.86
A_TSI_RESISTANCE_2	2.78

Figure 50 shows where the lowest safety factor is on the cylinder liner variant B1. The critical point is on the outside notch. The lowest safety factor is on the side of the exhaust valves because of the higher temperatures. The minimum safety factor of the variant B1 TSI is 2.36. This calculation proved that the proposed cylinder liner variant B1 made from EN-GJL-350 can be used.

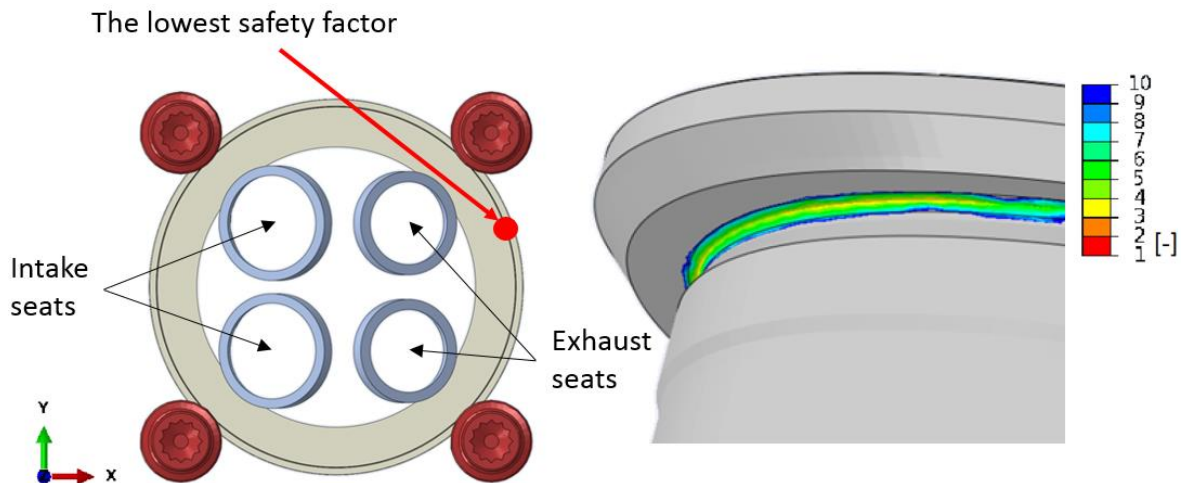


Figure 50: Cylinder Liner B1 Minimum Safety Factor

Table 22 shows the minimum cylinder liner variant B1 safety factors.

Table 22: Cylinder Liner B1 Minimum Safety Factor

Cylinder Liner Variant B1	Minimum Safety Factor [-]
B1_MPI	5.45
B1_TSI	2.36

Figure 51 shows where the lowest safety factor is on the cylinder liner variant B2. The critical point is also on the outside notch as in variant B1. The lowest safety factor is on the side of the exhaust valves because of the higher temperatures. The minimum safety factor of the variant B2 TSI is 3.18. This calculation proves that the proposed cylinder liner variant B1 made from EN-GJL-350 can be used.

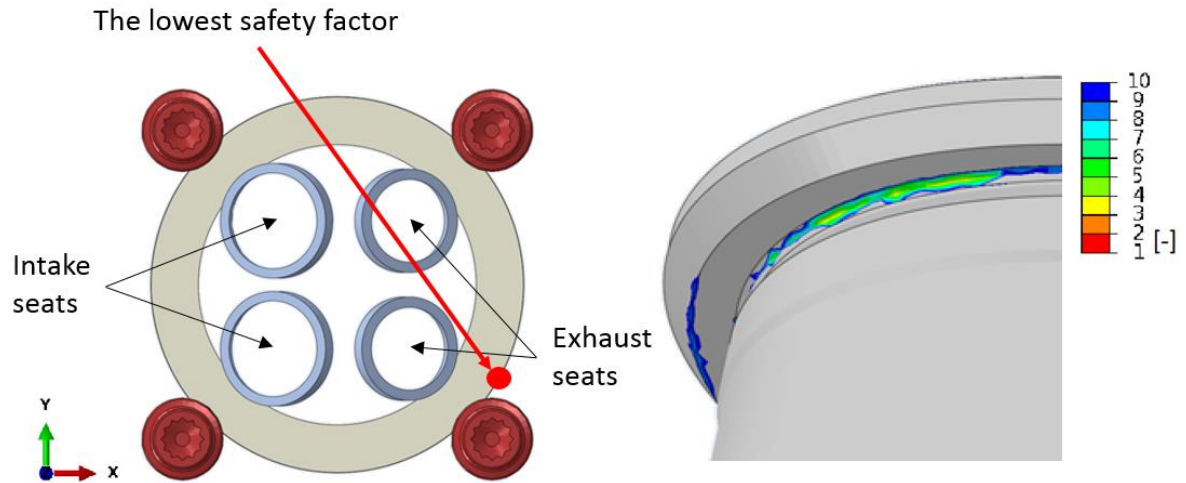


Figure 51: Cylinder Liner B2 Minimum Safety Factor

Table 23 shows the minimum cylinder liner variant B1 safety factors.

Table 23: Cylinder Liner B2 Minimum Safety Factor

Cylinder Liner Variant B2	Minimum Safety Factor [-]
B2_MPI	5.76
B2_TSI	3.18

### 4.10 Cumulative Plastic Deformation of Engine Parts

The stress of some engine components exceeded the yield strength. The magnitude of the plastic deformations was calculated. The plastic deformation must not be higher than the elongation strength for the material. This ensures unchanged material behavior. It is important to determine when the plastic deformation occurred. In our case, it is important that the plastic deformation occurs after the assembly or the first warm-up of the engine to the operating temperature. If the plastic deformation arises as a result of the ignition of the mixture in the cylinder, there is a risk that the behavior of the material will change every time the engine is started.

#### 4.10.1 Cumulative Plastic Deformation of the Cylinder Head

Figure 52 shows the magnitude of the plastic deformation of the cylinder head. The largest plastic deformation occur under the screw head. Plastic deformation occurs in all variants, after initial engine warm-up. The highest value of plastic deformation occurred in A TSI Resistance 2 variant. All achieved values are within the limits that do not affect the behavior of the material.

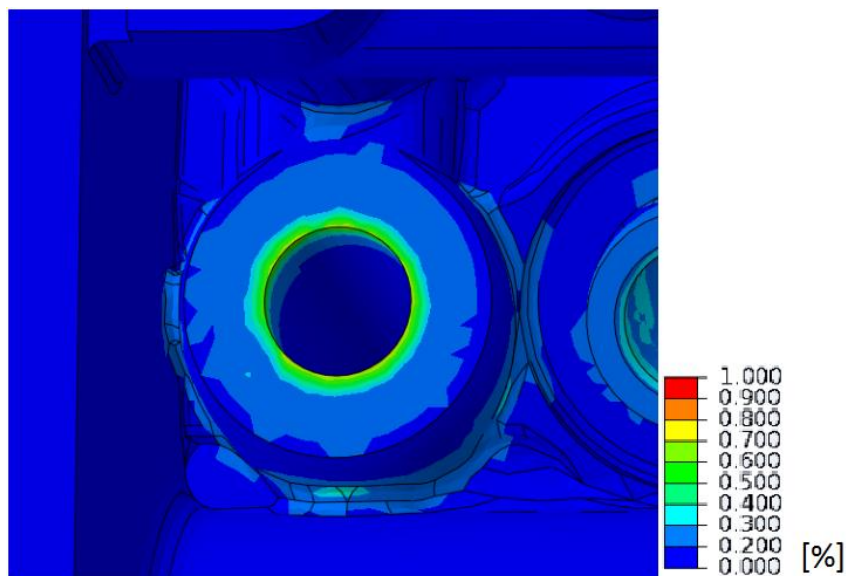


Figure 52: Plastic Deformation of the Cylinder Head A TSI Resistance 2

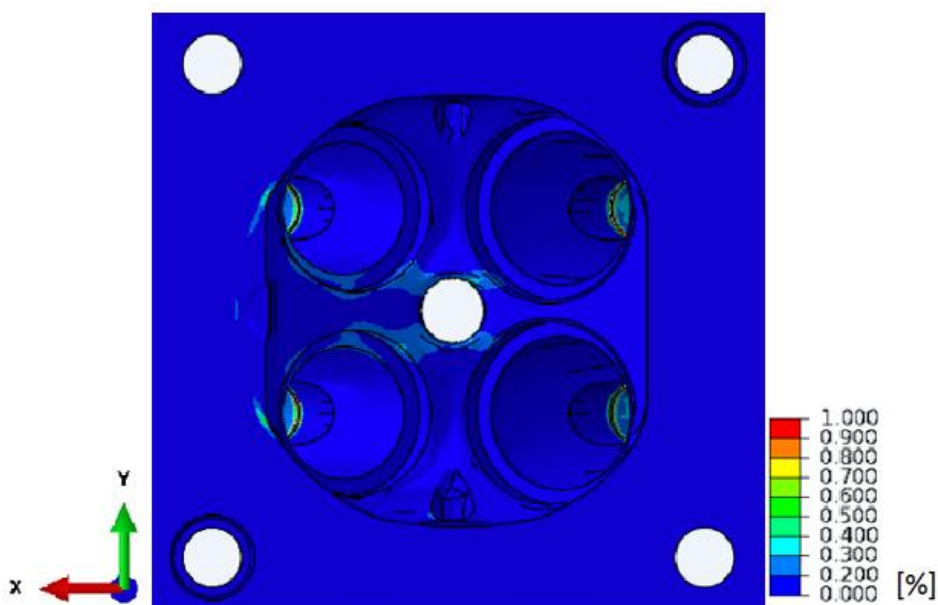


Figure 53: Plastic Deformation of the Cylinder Head A TSI Resistance 2 - 2

Table 24 shows the maximum cumulative plastic deformations of the cylinder head.

Table 24: Cylinder Head - Maximum Plastic Deformation

Cylinder Head	Maximum Plastic Deformation [%]
A_MPI_IDEAL_CONTACT	0.60
A_MPI_RESISTANCE_1	0.60
A_MPI_RESISTANCE_2	0.63
B1_MPI	0.59
B2_MPI	0.60
A_TSI_IDEAL_CONTACT	0.73
A_TSI_RESISTANCE_1	0.72
A_TSI_RESISTANCE_2	0.76
B1_TSI	0.73
B2_TSI	0.73

### 4.10.2 Cumulative Plastic Deformation of the Cylinder Liner

The elongation strength of the material EN-GJL-350 is from 0.3 to 0.8 [%].

[10]

Figure 54 shows the magnitude of plastic deformation of the cylinder liner variant A TSI Resistance 2. The largest plastic deformations occur on the outside notch on the side of the exhaust valves, close to the screw. The reason for the plastic deformation at this location is above all the high temperature.

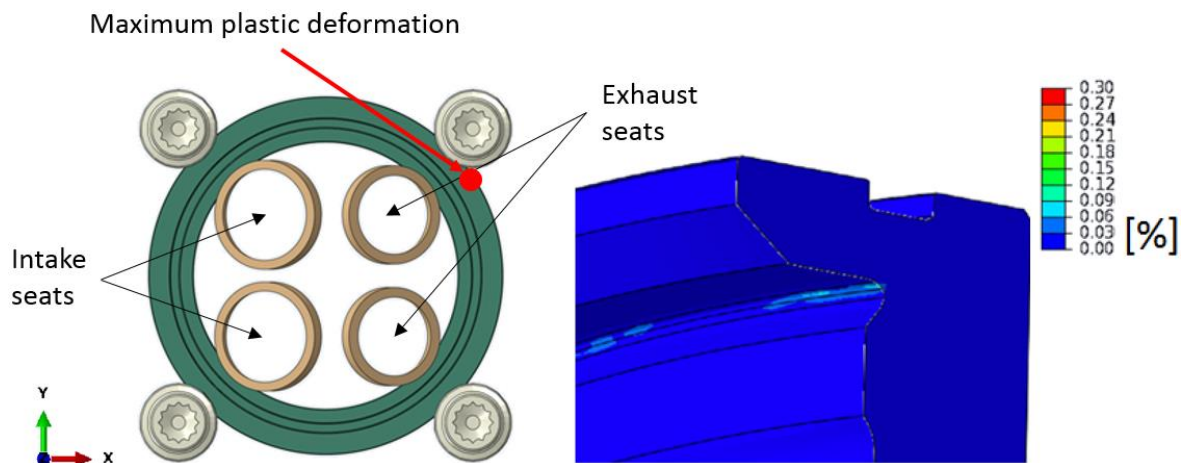


Figure 54: Cylinder Liner A TSI Resistance 2 Plastic Deformation

Table 25 shows the maximum cumulative plastic deformations of the cylinder liner variant A. All achieved values are within limits that do not affect the behavior of the material.

Table 25: Cylinder Liner A Maximum Plastic Deformation

Cylinder Liner Variant A	Maximum Plastic Deformation [%]
A_MPI_IDEAL_CONTACT	0.02
A_MPI_RESISTANCE_1	0.03
A_MPI_RESISTANCE_2	0.04
A_TSI_IDEAL_CONTACT	0.06
A_TSI_RESISTANCE_1	0.07
A_TSI_RESISTANCE_2	0.08

Figure 55 shows the magnitude of plastic deformation of the cylinder liner variant B1 TSI. The largest plastic deformation occurs on the outside notch on the side of the exhaust valves. The reason for the plastic deformation at this location is above all the high temperature as in the variant A.

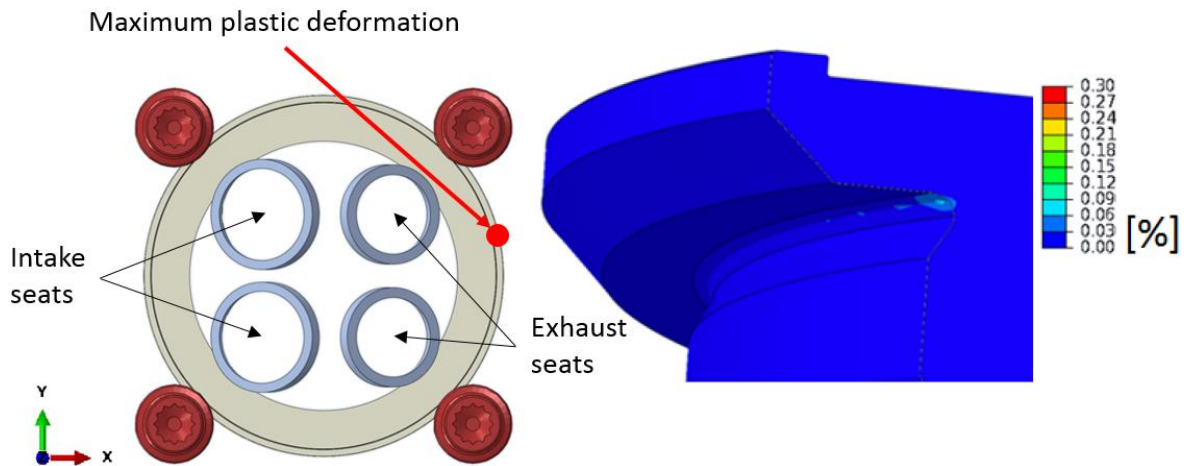


Figure 55: Cylinder Liner B1 TSI Plastic Deformation

Table 26 shows the maximum cumulative plastic deformations of the cylinder liner variant B1. All achieved values are within limits that do not affect the behavior of the material.

Table 26: Cylinder Liner B1 Maximum Plastic Deformation

Cylinder Liner Variant B1	Maximum Plastic Deformation [%]
B1_MPI	0.03
B1_TSI	0.07

Figure 56 shows the magnitude of plastic deformation of the cylinder liner variant B2 TSI. The largest plastic deformation occur at the same place as in variant B1 by the same reasons.

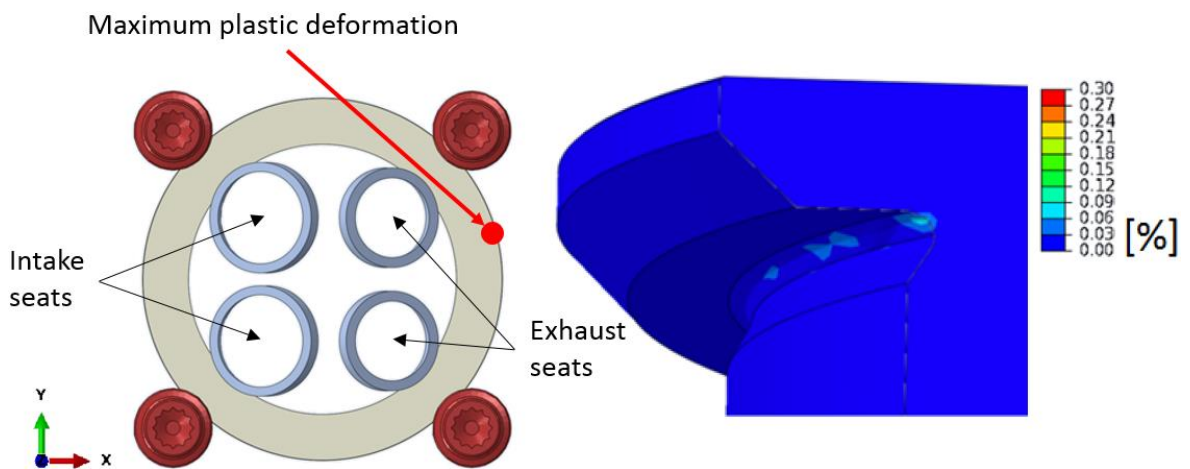


Figure 56: Cylinder Liner B2 TSI Plastic Deformation

Table 27 shows the maximum cumulative plastic deformations of the cylinder liner variant B2. All achieved values are within limits that do not affect the behavior of the material.

Table 27: Cylinder Liner B2 Maximum Plastic Deformation

Cylinder Liner Variant B2	Maximum Plastic Deformation [%]
B2_MPI	0.04
B2_TSI	0.08



## Chapter 5: Conclusion

This diploma thesis was part of a larger project that dealt with the design of the new single-cylinder petrol engine that will be used in the laboratory. The aim of this diploma thesis was to design an appropriate cylinder head gasket.

The preliminary design of the engine block, cylinder head and cylinder liner were available at the beginning of this thesis. These CAD data were modified in the Creo Parametric 2.0 software, with respect to a change in the geometry of the various proposed solutions.

The combustion chamber and the water are sealed using Viton O-rings in the first variant. In the other two variants, the combustion chamber is sealed using the copper gasket and the water is sealed using the Viton O-ring as in the first variant. The highest O-ring temperature is achieved in Variant A. The highest O-ring temperature reaches 208 °C. The manufacturer of the O-ring guarantees that the desired properties are maintained till the temperature 250 °C. The maximum clearance of the sealing surfaces achieved 0.004 mm. The manufacturer guarantees sealing of the pressure at a maximum clearance of 0.1 mm.

Stress analysis of the gaskets, modified parts of engine and cylinder head was performed in the software Abaqus. FEMFAT safety calculations were performed for all variants of the cylinder liner. The calculation of cumulative plastic deformations was performed, where the yield strength was exceeded. The highest cumulative deformation of the cylinder head was 0.76 % in the variant A. The amount of cumulative plastic deformations must not exceed 1 % in the cylinder head because of maintaining the required mechanical properties of the material AlSi10Mg. The highest cumulative deformation of the cylinder liner was 0.08 % in the variants A and B2. The amount of cumulative plastic deformations must not exceed 0.3 % in the cylinder liner because of maintaining the required mechanical properties of the material EN-GJL-350.

The safety factor and required prestressing of the cylinder head screws was calculated with respect to the maximum combustion pressure. This safety factor has been verified by the FEMFAT software calculation. The safety factor of the screw, which was calculated by analytical calculation, is 2.45. The lowest safety factor which was calculated using FEMFAT came out for variant B2 with a value of 2.35. The lowest safety factor of the cylinder liner which was calculated using FEMFAT came out for variant B1 with a value of 2.36. The lowest possible safety factor of the screw and the cylinder liner which can be considered as permissible is 1.3.

All versions of the gasket, modified engine parts and proposed cylinder head screws can be used to construct the engine, taking into account the temperature, stress and safety results of the calculations.

## Cited Literature

- [1] SCEGASKETS [online]. [Citation: 25 3 2017]. Available: [http://scegaskets.com/wp\\_super\\_faq/whats-what-the-facts-of-gasket-materials/](http://scegaskets.com/wp_super_faq/whats-what-the-facts-of-gasket-materials/)
- [2] RUBENA [online]. [Citation: 13 3 2017]. Available: <http://www.rubena.cz/cz/>
- [3] Eagleson, J. S., Head Gasket Finite Element Model Correlation, University of Windsor, 2013.
- [4] ElringKlinger [online]. [Citation: 7 4 2017]. Available: <https://files.vogel.de/vogelonline/vogelonline/companyfiles/1399.pdf>
- [5] OICA [online]. [Citation: 18 3 2017]. Available: <http://www.oica.net/wp-content/uploads//ranking2015.pdf>
- [6] HENNLICH [online]. [Citation: 13 4 2017]. Available: <https://www.hennlich.cz/produkty/tesneni-o-krouzky-356.html>
- [7] Dillinger, J. a kolektiv, Moderní strojírenství pro školu i praxi, Europa Sabotáles.
- [8] COG [online]. [Citation: 3 5 2017]. Available: <http://www.cog.de/en/o-rings-products/o-ring-basics.html>
- [9] Doc. Ing. Vladimír Švec, CSc., Části a mechanismy strojů – příklady, Praha: České vysoké učení technické v Praze, 2008.
- [10] SN Cast Iron [online]. [Citation: 12 6 2017]. Available: [http://www.sn-castiron.nl/en//castiron/en\\_gjl.html](http://www.sn-castiron.nl/en//castiron/en_gjl.html)
- [11] Getting Started with Abaqus Interactive Edition [online]. [Citation: 1 6 2017]. Available: <http://abaqus.software.polimi.it>
- [12] Kustom1warehouse [online]. [Citation: 2 3 2017]. Available: [https://www.kustom1warehouse.net/Copper\\_head\\_shims\\_for\\_VW\\_Volkswagen\\_p/copperheadgasket.htm](https://www.kustom1warehouse.net/Copper_head_shims_for_VW_Volkswagen_p/copperheadgasket.htm)
- [13] FR.Sport [online]. [Citation: 15 3 2017]. Available: [http://www.frsport.com/Cometic-H1794SP3030S-Nissan-SR20VE-88mm-x--030--MLS-Head-Gasket\\_p\\_26509.html](http://www.frsport.com/Cometic-H1794SP3030S-Nissan-SR20VE-88mm-x--030--MLS-Head-Gasket_p_26509.html)
- [14] Uniaxial Tension and Compression Testing of Materials [online]. [Citation: 5 7 2017]. Available: <https://www.researchgate.net/file.PostFileLoader.html?id=57a2ce675b4952c7610cabc1&assetKey=AS%3A391228131692544%401470287463211>
- [15] E-konstruktor [online]. [Citation: 1 7 2017]. Available: <https://e-konstruktor.cz/prakticka-informace/hodnoty-mezipevnosti-kluzu-unavy-a-dovolenych-napeti-pro-ocel>

## List of Figures

Figure 1: Engine Model .....	14
Figure 2: Design Process of the Gasket [3] .....	15
Figure 3: Composite Head Gasket [1] .....	16
Figure 4: MLS Cross-section [4] .....	17
Figure 5: MLS Head Gasket [13].....	18
Figure 6: Copper Head Gasket [12].....	19
Figure 7: Acting of Operating Pressure [2] .....	20
Figure 8: Dimensions of the O-ring [2] .....	20
Figure 9: Rectangular Groove [2].....	21
Figure 10: Triangular Installation Space [8] .....	21
Figure 11: Axial Compression [6] .....	23
Figure 12: Mounting Preload [9].....	28
Figure 13: Variant A .....	33
Figure 14: Variant B1 .....	34
Figure 15: Variant B2 .....	35
Figure 16: Engine Block.....	38
Figure 17: Cylinder Head.....	39
Figure 18: O-ring 96x2 .....	40
Figure 19: Screw M9x100 .....	40
Figure 20: Intake Valve Seat (left) and Exhaust Valve Seat .....	41
Figure 21: Cylinder Liner A.....	42
Figure 22: Intake Valve Guide (left) and Exhaust Valve Guide .....	43
Figure 23: Copper Gasket.....	43
Figure 24: Valve Seats and Valve Guides Pressed into the Cylinder Head .....	44
Figure 25: Stress after Tightening to the Desired Preload .....	45
Figure 26: Stress during the Highest Combustion Pressure Variant A TSI Resistance 2 .....	46
Figure 27: Contact Pairs in the Computational Model .....	48
Figure 28: Tie Contact Pair.....	49
Figure 29: Contact Pair of the Valve Seats and the Valve Guides .....	49
Figure 30: Contact Pair Cylinder Liner - Engine Block.....	50
Figure 31: Temperature Field of the Engine Variant B1 TSI .....	53
Figure 32: Contacts Containing Thermal Resistances.....	55
Figure 33: O-ring Combustion A TSI Resistance 2.....	56
Figure 34: Cylinder Liner A TSI Resistance 2 Temperature.....	58
Figure 35: Cylinder Liner B1 TSI Temperature .....	60
Figure 36: Cylinder Liner B2 TSI Temperature .....	60
Figure 37: Set of Elements Loaded by the Combustion Pressure.....	61
Figure 38: Groove for the O-ring of the Sealing Combustion Chamber .....	62
Figure 39: Stress of the Cylinder Head A TSI Resistance 2 .....	64
Figure 40: Contact Pressure between the Cylinder Head and the Copper Gasket .....	65

---

Figure 41: Stress of the Cylinder Liner A TSI Resistance 2 .....	66
Figure 42: Stress of the Cylinder Liner B1 TSI .....	67
Figure 43: Cylinder Liner B1 TSI Contact Pressure .....	68
Figure 44: Stress of the Cylinder Liner B2 TSI .....	69
Figure 45: Cylinder Liner B2 TSI Contact Pressure .....	70
Figure 46: Stress of the Copper Gasket .....	71
Figure 47: Stress of the Engine Block .....	71
Figure 48: Cylinder Head Screw Minimum Safety Factor .....	73
Figure 49: Cylinder Liner A Minimum Safety Factor .....	74
Figure 50: Cylinder Liner B1 Minimum Safety Factor .....	75
Figure 51: Cylinder Liner B2 Minimum Safety Factor .....	76
Figure 52: Plastic Deformation of the Cylinder Head A TSI Resistance 2 .....	77
Figure 53: Plastic Deformation of the Cylinder Head A TSI Resistance 2 - 2 .....	77
Figure 54: Cylinder Liner A TSI Resistance 2 Plastic Deformation .....	78
Figure 55: Cylinder Liner B1 TSI Plastic Deformation .....	79
Figure 56: Cylinder Liner B2 TSI Plastic Deformation .....	80

## List of Tables

Table 1: Operating Temperatures of the O-ring Materials [6] .....	21
Table 2: Comparison of Gasket Types .....	24
Table 3: Numbers and Types of Elements .....	43
Table 4: Boundary Conditions Summary .....	47
Table 5: Contacts Overview .....	51
Table 6: Coolant Parameters .....	54
Table 7: Summary of the Computational Variants .....	56
Table 8: O-ring Temperatures Variant A.....	57
Table 9: O-ring Temperatures Variant B1.....	57
Table 10: O-ring Temperatures Variant B2.....	57
Table 11: Cylinder Liner A Temperature .....	59
Table 12: Cylinder Liner B1 Temperature .....	59
Table 13: Cylinder Liner B2 Temperature .....	59
Table 14: Combustion Chamber Pressures.....	62
Table 15: Lift the Cylinder Head Relative to the Cylinder Liner.....	63
Table 16: Maximum Stress of the Cylinder Head from the Screw .....	64
Table 17: Maximum Stress of the Cylinder Liner A .....	67
Table 18: Maximum Stress of the Cylinder Liner B1.....	68
Table 19: Maximum Stress of the Cylinder Liner B2.....	69
Table 20: Cylinder Head Screw Minimum Safety Factor .....	73
Table 21: Cylinder Liner A Minimum Safety Factor .....	74
Table 22: Cylinder Liner B1 Minimum Safety Factor .....	75
Table 23: Cylinder Liner B2 Minimum Safety Factor .....	76
Table 24: Cylinder Head - Maximum Plastic Deformation .....	78
Table 25: Cylinder Liner A Maximum Plastic Deformation .....	79
Table 26: Cylinder Liner B1 Maximum Plastic Deformation .....	80
Table 27: Cylinder Liner B2 Maximum Plastic Deformation .....	80

## List of Charts

Chart 1: Heat Release .....	13
Chart 2: Load Characteristics of Viton O-ring .....	22
Chart 3: Stress-strain Diagram of the AISi10Mg .....	39
Chart 4: Thermal Expansion of the 30CrNiMo8.....	40
Chart 5: Modulus of Elasticity of the 30CrNiMo8.....	41
Chart 6: Stress-strain Diagram of the GJL 350.....	42

## List of Attachments

Attachment 1: Drawing documentation of the design of three sealing variants